

---

## Community structure of deep-sea benthic metazoan meiofauna in the polymetallic nodule fields in the eastern Clarion-Clipperton Fracture Zone, Pacific Ocean

Jia Wen Tong Samantha <sup>1,2,\*</sup>, Qi Gan Bin <sup>1</sup>, Siang Tan Koh <sup>1,2</sup>

<sup>1</sup> Tropical Marine Science Institute, National University of Singapore, 18 Kent Ridge Road, Singapore, 119227

<sup>2</sup> Keppel-NUS Corporate Laboratory, Faculty of Engineering, National University of Singapore, Blk E1A, #03-03, 1 Engineering Drive 2, Singapore, 117576

\* Corresponding author : Samantha Jia Wen Tong, email address : [tmstjws@nus.edu.sg](mailto:tmstjws@nus.edu.sg)

---

### Abstract :

The abyssal sea floor of the Clarion-Clipperton Fracture Zone (CCFZ) in the Pacific Ocean is expected to become a commercially important nodule mining area in the near future. Hence, it is crucial to understand the community structure of biological communities there, so that nodule harvesting activities can be designed to minimize deleterious impacts on marine life. Meiofauna is an important component of the abyssal infaunal community but relatively little is known on their biodiversity, abundance, and community structure in the CCFZ. We provide here the first quantitative observations of metazoan benthic animals  $\geq 40 \mu\text{m}$  in a  $30 \times 30 \text{ km}$  area survey stratum in the Ocean Mineral Singapore contract area at the eastern end of the CCFZ. A total of 88 867 individuals, identified to 23 animal groups, were collected from 12 randomly sampled stations using a multiple corer. Even in our small surveyed area, the meiofaunal community structure appeared different at our stations, confirming that the CCFZ deep sea floor is very diverse. From the top 0–5 cm sediment layer, unsurprisingly, the three most abundant animal groups were the Nematoda ( $87.9 \pm 2.9\%$ ), the Nauplii ( $5.0 \pm 1.3\%$ ) and the Copepoda ( $4.3 \pm 1.1\%$ ). The majority of the meiobenthos (76.6%) were in the top 0–2 cm sediment layer. Our results suggested that substratum shear strength was negatively and significantly correlated to meiofaunal abundances among the 12 stations. Nodule cover and nodule volume did not appear to affect the meiofaunal community structure at the major taxon level. The mean meiofaunal abundance ( $235.7 \pm 26.4 \text{ ind./10 cm}^2$ ) was relatively high at our site in comparison with previous studies elsewhere in the CCFZ, further confirming the westward decrease in meiofaunal abundance across the CCFZ.

### Highlights

► Provides the first quantitative description of meiofaunal composition in the OMS contract area (eastern CCFZ). ► Community structure was different at 12 stations in a  $30 \times 30 \text{ km}$  area, showing that meiofauna in the CCFZ is very diverse. ► Substratum shear strength was significantly associated with differences

---

in meiofaunal abundance and community structure. ► Our findings reiterate the decreasing westward trend of meiofaunal abundance in the CCFZ.

**Keywords** : Meiobenthos, Polymetallic nodule mining, Abyssal benthos, ABYSSLINE 02

45

46

## 1. INTRODUCTION

47

48

The Clarion-Clipperton Fracture Zone (CCFZ) refers to an area of about six million square kilometres located in the eastern Pacific Ocean, bounded by the Clarion Fracture Zone to the north and the Clipperton Fracture Zone to the south. The CCFZ is considered as one of the largest reservoirs for high-grade polymetallic nodules, containing commercially valuable metals such as manganese, copper, nickel and cobalt (Hein et al., 2013; Lodge et al., 2014). Compared to a few decades ago, advances in technology now have made deep-sea mining a realistic option to meet the increasing global demand for these metals. Besides, some metals can even be found more abundantly in the CCFZ than in terrestrial reserves (Hein et al., 2013). As a result, mining for nodules from the CCFZ has gained international interest.

55

56

Harvesting polymetallic nodules from the sea floor will undoubtedly affect the abyssal marine environment. A key consequence of mining activities is habitat destruction and the loss of animals living on and within nodules, as well as in the sediment. Sediment plumes arising from the mining process will further result in a large-scale smothering of habitats (Rolinski et al., 2001; reviewed in Allsopp et al., 2013). Previous disturbance studies, although conducted on a small spatial scale compared to the foreseeable extent of seabed mining, have demonstrated lasting changes in the abundance and composition of fauna, and exacerbated by long recovery times especially for sessile taxa reliant on hard-substrata (Bluhm et al., 1995; Bluhm, 2001; Miljutin et al., 2011, 2015; Stratmann et al., 2018). Disturbance tracks were

57

58

59

60

61

62

also still visible after many years (e.g., after 26 years in Miljutin et al., 2011). To minimise serious environmental harm, it is very important to first study the deep-sea biodiversity of the largely unexplored CCFZ before mining commences, since having baseline data is the first and necessary step to carry out future comparisons, disturbance and recovery studies. These studies will be critical in developing strategic mining plans or techniques having the least impact to the marine environment, towards striking a good balance between conservation and exploitation. Unfortunately, deep-sea baseline data are not extensively available due to the massive expanse of the deep seabed and high costs incurred for deep-sea expeditions, resulting in fewer sampling efforts compared to shallower waters. Hence, relatively little is known about the ecology and biogeography of deep-sea fauna in general (Sinniger et al., 2016).

The International Seabed Authority (ISA) was set up in 1994 under the United Nations Convention on the Law of the Sea (UNCLOS) to manage seabed mining outside the limits of national jurisdiction, including the CCFZ. The first CCFZ exploration contract was granted in 2001, with 19 international contracts to date (ISA, 2022). In January 2015, ISA granted a 15-year seabed exploration contract for polymetallic nodules to Ocean Mineral Singapore, a subsidiary of Keppel Corporation Limited. Under this contract, a 58,280 square kilometre exploratory site in the eastern part of the CCFZ was allocated to Singapore. It is a requirement for every contractor to gather environmental baseline data in order to develop environmental impact assessments as well as implement suitable environmental monitoring and management plans (ISA, 2011, 2013). Previous expeditions to various contract areas have generated new insights on the biology, distribution, connectivity and structure of biological communities (e.g., Janssen et al., 2019; Sánchez et al., 2019; Simon-Lledó et al., 2020; De Smet et al., 2021, Laming et al., 2021, Wear et al., 2021); as well as numerous discoveries of species new to science (e.g., Bonifácio & Menot, 2019; Bai et al., 2020; Gooday et al., 2020; Malyutina et al., 2020), highlighting the importance of carrying out such environmental studies there.

In February 2015, Ocean Mineral Singapore (OMS) and United Kingdom Seabed Resources Limited (UKSRL) set out on a joint research expedition—Abyssal Baseline Project 2015 (ABYSSLINE 02/AB02), which was designed according to ISA's environmental guidelines (ISA, 2013). The aim of ABYSSLINE 02, in terms of improving the biological knowledge in the OMS site, was to conduct a biological baseline by characterising and quantifying the biodiversity in the OMS site. This expedition was very successful and 29 papers which included biological data from this area have been published so far (Table 1 and references therein). These papers covered all benthic size groups (i.e., micro-, meio-, macro- and megafauna) as well as the pelagic larval assemblages, and new species descriptions (a brief description of each study is provided in Table 1).

**Table 1.**  
Brief description of studies that included biological data found in the OMS exploratory area.

Study	Organism group	Sampling device	Brief description
Amon et al., 2017	Animals found at sites of organic falls	AUV, ROV	First record of wood falls and second record of carcass falls in the CCFZ. One wood fall (only observed using AUV) and one cetacean fall (samples also collected using ROV) were found in the OMS area. Three other wood falls were found in the UKSRL and APEI regions. These observations confirm that wood fall can occur far from major land masses. Wood-boring xylophagaid bivalves and other associated fauna colonised these wood falls.
Chim & Tong, 2020	Tanaidacea	Box corer	Description of a new genus and species ( <i>Unispinosus eopacificus</i> ) and a new species in the genus <i>Portaratum</i> ( <i>P. birdi</i> ).
Chuar et al., 2020	Metazoan benthos larger than 250 µm	Box corer	Community structure of abyssal benthos collected using a box corer from 12 stations within the OMS area was presented. A total of 42 families of Polychaeta, 15 families of Copepoda, ten families of Tanaidacea and eight families of Isopoda were reported.
Cordier et al., 2022	Eukaryotic DNA metabarcodes obtained from deep ocean sediments	Multiple corer	This study collected deep ocean sediments collected during various expeditions, including from the OMS area. Eukaryotic DNA metabarcoding datasets were obtained and compared with published datasets from pelagic euphotic and aphotic zones. They found that the eukaryotic taxonomic composition from deep ocean sediment were different from, and at least threefold that of, pelagic realms.
Drennan et al., 2021	Annelida: Nereididae	Box corer, Multiple corer, Epibenthic sledge, ROV	Description of a new species of nereidid annelid, <i>Neanthes goodayi</i> . This species was found living in polymetallic nodule crevices, mudballs on nodule surfaces, or burrowing in xenophyophore Foraminifera that were growing on nodules.

Goineau & Gooday, 2019	Foraminifera	Multiple corer	A total of 580 morphospecies were reported from 11 samples. Foraminifera are one of the dominant benthic faunas in CCFZ.
Gooday & Goineau, 2019	Foraminifera	Multiple corer	Examined Foraminifera using finer sieve mesh sizes between 63–150 µm. A total of 462 morphospecies were reported from five samples. Monothalamids (mainly spheres, <i>Lagenammina</i> spp., <i>Nodellum</i> -like forms and saccamminids), rotaliids, hormosinids, trochamminids and textulariids were identified among the samples.
Gooday et al., 2017a	Foraminifera	Box corer, Multiple corer, Epibenthic sledge	Description of new species of Foraminifera from the genus <i>Aschemonella</i> .
Gooday et al., 2017b	Foraminifera	Box corer, Multiple corer, Epibenthic sledge	Abundance, diversity and distribution of xenophyophores were presented. Based on test morphology, 36 morphospecies, including 34 new species, were distinguished among 130 specimens. Molecular genetic data was also used to clarify the phylogenetic relationships of the xenophyophores.
Gooday et al., 2018a	Foraminifera	Box corer, Multiple corer, Epibenthic sledge	Description of new species of Foraminifera from the genus <i>Psammina</i> .
Gooday et al., 2018b	Foraminifera	Box corer, Multiple corer	Description of two new species of Foraminifera, <i>Tendalia reteformis</i> and <i>Bizzaria bryriformis</i> using samples collected from OMS.
Gooday et al., 2018c	Foraminifera	Box corer and multiple corer	CT imaging was used to examine the interstructure (granellare, test particles and stercomare) of Foraminifera from the genera <i>Psammina</i> and <i>Galatheammina</i> .
Gooday et al., 2021	Foraminifera	Multiple corer	The biodiversity and distribution of Foraminifera across the Clarion-Clipperton zone, including data from OMS exploratory area (Goineau & Gooday, 2019; Gooday & Goineau, 2019), was presented.
Guggolz et al., 2020	Annelida: Spionidae	Box corer, Epibenthic sledge	16S and 18S molecular markers were used to study the diversity and distribution patterns of spionid polychaetes from the genera <i>Prionospio</i> and <i>Aurospio</i> , from the tropical North Atlantic, Puerto Rico Trench and central Pacific (including specimens collected from the OMS area).
Kaiser et al., 2021	Isopoda	Epibenthic sledge	Five <i>Nannoniscus</i> species from five licence areas, including the OMS exploratory area, were described. The genetic variation, based on CO1 and 16S mtDNA, of <i>N. pedro</i> and <i>N. menoti</i> in the Clarion-Clipperton Fracture Zone, was found to be widespread.
Kersten et al., 2017	Larval assemblages	Plankton pump, sediment trap	The first description of the invertebrate meroplankton larval assemblage in the OMS and UKSRL areas was presented. Results from plankton pumps indicated that there was little variation in the meroplankton diversity and abundance but sediment traps samples showed that there was high temporal variability in vertical flux.
Kersten et al., 2019	Larval assemblages	Plankton pump	Pelagic larval assemblages (species richness, diversity, and spatial variability) were examined using tree-of-life (TOL) metabarcoding. They detected a diverse assemblage, including a number of taxa not previously reported at abyssal depths or within the Pacific Ocean. This method also found 2.7–4.3 times higher diversity when compared to morphology-based analyses.
Kristensen et al., 2019	Loricifera	Multiple corer	Undescribed loriciferans from the genera <i>Rugiloricus</i> and <i>Pliciloricus</i> were found nested in spherical agglutinated structures.
Leitner et al., 2017	Bait-attending animals	Baited camera	A detailed description of the bait-attending community of the CCFZ was documented for the first time. The taxa found were <i>Bassozetus</i> sp., <i>Bathyonus caudali</i> , <i>Coryphaenoides</i> spp., <i>Histiobranchus bathybius</i> , <i>Pachycara nazca</i> , Zoarcidae sp. 2, <i>Plesiopenaeus armatus</i> , <i>Hymenopenaeus nereus</i> , and <i>Ophiomusium</i> cf. <i>glabrum</i> .

Lejzerowicz et al., 2021	Microbial and meiofaunal eukaryotes	Multiple corer	DNA and RNA metabarcoding, targeting microbial and meiofaunal eukaryotes, were conducted on sediment samples from the CCFZ as well as other abyssal regions.
Lim et al., 2017	Porifera	Box corer	Description of a new genus and species of sponge, <i>Plenaster craigi</i> .
Lindh et al., 2017	Bacteria	Conductivity, temperature, depth (CTD) rosette equipped with Niskin sampling bottles, Box corer, Multiple corer	Examined bacterial communities in the water column, nodule habitats, and sediment habitats in the OMS and UKSRL areas.
Lindh et al., 2018	Bacterioplanktonic community	16S rRNA amplicons obtained in Lindh et al. (2017)	This study used 16S rRNA amplicons of bacterioplanktonic community composition from the CCFZ, as well as global ocean 16S rRNA gene data, to predict the response of mining impacts on the bacterioplanktonic community. They found that the release of sediment plumes in the epi- and mesopelagic waters could change the microbial community structure.
Mohrbeck et al., 2021	Amphipoda	Baited trap	Ten amphipod species were morphologically identified from four areas (UK-1 Stratum A, UK-1 Stratum B, OMS-1 Stratum A, APEI-6). Mitochondrial COI sequences, however, were grouped into 12–24 MOTUs or putative species. Potential cryptic diversity were found in two species morphologically identified as <i>Paralicella caperesca</i> and <i>Valettietta cf. anacantha</i> .
Sweetman et al., 2019	Bacteria, microbial community, macrofauna	Deep-sea benthic chamber lander	Pulse-chase experiments were used to quantify the cycling of carbon in the CCFZ, which found that benthic macrofauna played a minor role, while benthic bacteria dominated phytodetritus consumption in short-term C-cycling processes.
Taboada et al., 2018	Porifera	Box corer, Multiple corer, Epibenthic sledge, Agassiz trawl, ROV	Investigated the population connectivity of an abyssal demosponge, <i>Plenaster craigi</i> . This study suggested that APEI-6 is inadequate on its own as a propagule source for <i>P. craigi</i> for the entire eastern CCFZ.
Washburn et al., 2021	Macrofauna	Box corer	Collated macrofaunal biodiversity data sets from eight studies, including data from Chuar et al. (2020). Macrofaunal abundance and diversity across the CCFZ differed substantially; many species were singletons or doubletons; and most species were new to science.
Wear et al., 2021	Bacteria, Archaea	ABO2 samples were resequenced from Lindh et al. (2017)	16S ribosomal RNA was used to characterise abyssal bacterial and archaeal communities. In the CCFZ, an east and west distinction in the nodule microbial community composition can be observed, although the magnitude was small.
Wiklund et al., 2019	Annelida: Capitellidae, Opheliidae, Scalibregmatidae, Traviidae	Box corer, Multiple corer, Epibenthic sledge, ROV	Some 23 species of Annelida were described with specimens collected from the UK-1, OMS-1 and APEI-6 areas.
This study	Meiofauna (metazoan benthos larger than 40 µm)	Multiple corer	First quantitative description of the community structure of abyssal benthos above 40 µm collected using the multiple corer from 12 stations within the OMS area.

97  
 98 Even with these informative papers, the overall picture of the biodiversity at the OMS site is not yet complete and is  
 99 still missing a crucial component—the metazoan meiofaunal community. The metazoan meiofauna, which we defined  
 100 as animals retained on a 40 µm sieve in this paper, represent the most abundant and diverse group of benthic metazoan  
 101 animals in the deep sea. Meiofauna can influence ecosystem processes such as mineralization of organic matter, nutrient  
 102 recycling, sustaining energy flow between trophic levels—overall maintaining a healthy benthic ecosystem  
 103 (Nascimento et al., 2012; Bonaglia et al., 2014; Schratzberger & Ingels, 2018). Moreover, their small sizes, high  
 104 abundance, lack of larval dispersion, high lifecycle turnover, and recolonization rates (Gerlach, 1971; Giere, 2009),  
 105 allow the meiofauna to potentially serve as biological indicators in the event of any disturbances. As one of the key  
 106 components of the benthic ecosystem, it is important to include meiofauna while considering deep-sea monitoring  
 107 (Ingels et al., 2021).

108  
 109 A number of meiofaunal studies have already been done in the CCFZ. Meiofaunal abundance and composition data  
 110 were collected during various scientific cruises to different contractor areas such as the Federal Institute for  
 111 Geosciences and Natural Resources (BGR), Germany (Hauquier et al., 2019; Uhlenkott et al., 2020); Global Sea  
 112 Mineral Resources NV (GSR), Belgium (Hauquier et al., 2019, Pape et al., 2017, 2021); Institut Français de Recherche

113 pour l'Exploitation de la Mer (IFREMER), France (Mahatma, 2009; Hauquier et al., 2019); Interoceanmetal Joint  
 114 Organization (IOM) (Radziejewska & Modlitba, 1999; Radziejewska et al., 2001; Radziejewska, 2002, 2014); and the  
 115 Korea Deep Ocean Study area (KODOS) (Kim et al., 2000, 2004; Min et al., 2004, 2018). New meiofaunal species have  
 116 also been described from these contract areas—Harpacticoida from GSR (Gheerardyn & George, 2019), BGR, IOM and  
 117 IFREMER (Mercado-Salas et al., 2019) and the Korean contract area (Cho et al., 2016), Tardigrada from the Chinese  
 118 contract area (Bai et al., 2020), Loricifera (Fujimoto & Murakami, 2020) and Nematoda from Japanese contract area  
 119 (DORD) (Shimada et al., 2020). Multiple expeditions to the same contract area allow comparison studies of temporal  
 120 and spatial trends (Pape et al., 2017; Uhlenkott et al., 2020), recovery studies by examining changes before and after  
 121 disturbances (Radziejewska et al., 2001; Radziejewska, 2002; Fukushima et al., 2022), and the synthesis of meiofauna  
 122 diversity in the CCFZ by using data across the various contract areas (e.g., Kinorhyncha diversity in Sánchez et al.,  
 123 2019; Nematoda distribution in Hauquier et al., 2019). As ABYSSLINE 02 was the first cruise to the OMS contract  
 124 area, there is, naturally, a lack of data on meiofauna from OMS before this expedition. Apart from a description of  
 125 Loricifera inside spherical agglutinated structures (Kristensen et al., 2019) and sediment DNA and RNA barcodes  
 126 obtained (Lejzerowicz et al., 2021), all published papers from OMS so far only included metazoan animals of  $>250\ \mu\text{m}$   
 127 (Table 1). A quantitative baseline of the benthic metazoan meiofauna is imperative to obtain a better perspective of the  
 128 biodiversity in the area. This paper aims to close this knowledge gap.

129

## 130 2. MATERIALS & METHODS

131

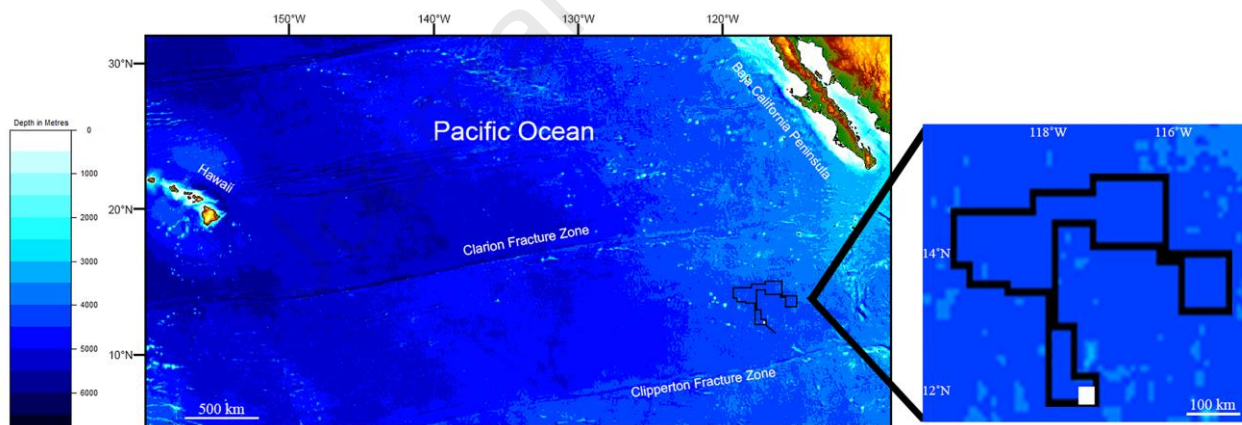
### 132 2.1. Study area

133

134 All samples were collected during the research cruise ABYSSLINE 02, on board the research vessel Thomas G.  
 135 Thompson (T-AGOR-23), between 16 February to 22 March 2015 in the eastern CCFZ (Fig. 1). Within a  $30 \times 30\ \text{km}$   
 136 area in the southernmost region of OMS contract area (centered at  $12^\circ 8.2'\ \text{N}$ ,  $117^\circ 17.7'\ \text{W}$ ), at depths of between  
 137 4000–5000 m (Fig. 1), 12 stations were randomly selected for sampling (Fig. 2). Photographs taken from autonomous  
 138 underwater vehicle (AUV) and box corer deployments showed that the seafloor is covered with polymetallic nodules,  
 139 often covering more than 30% of the box corer ( $50 \times 50\ \text{cm}$ ) surface area. Multibeam bathymetry showed that the OMS  
 140 study area was almost devoid of seamounts, and the 900 square kilometer region sampled in this study was mainly  
 141 dominated by low relief NNW-SSE lineated ridges and troughs (Chuar et al., 2020).

142

143



144

145 **Fig. 1.** Map of the Clarion-Clipperton Fracture Zone (CCFZ). Location of Ocean Mineral Singapore (OMS) exploration contract area is outlined in  
 146 black lines. The  $30 \times 30\ \text{km}$  surveyed area during ABYSSLINE 02 research expedition is indicated by the small white box. Figure reproduced and  
 147 modified from Chuar et al. (2020).

148

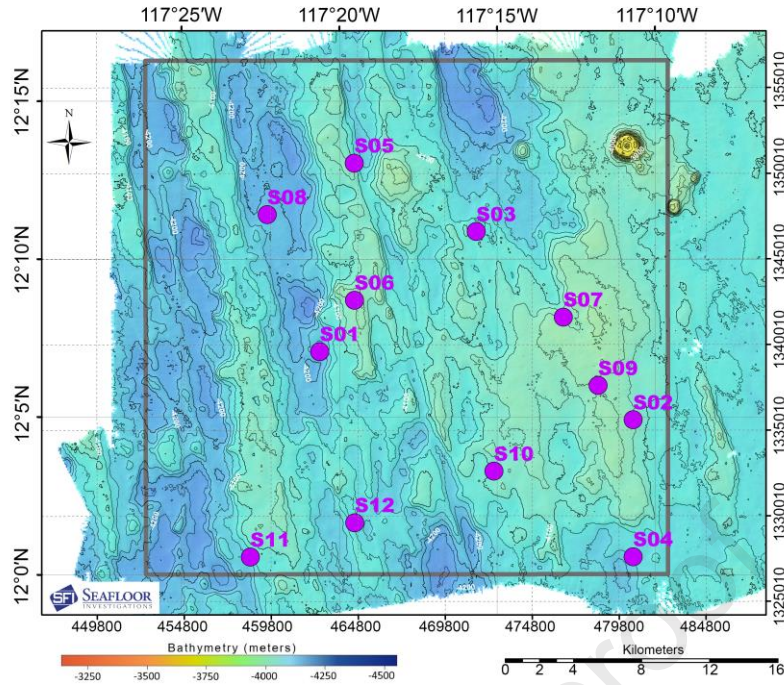


**Fig. 2.** Twelve randomly assigned stations within the 30 × 30 km surveyed area of the Ocean Mineral Singapore (OMS) exploration contract area. A Mega Multiple Corer was deployed once at each station during the ABYSSLINE 02 research expedition from 24 Feb.–17 Mar. 2015. This figure taken from Chuar et al. (2020) was modified from the map created by Seafloor Investigations LLC for the ABYSSLINE Project using ArcGIS software.

## 2.2. Sample collection

At each of the 12 stations a Mega Multiple Corer (OSIL) was deployed once, which collected 12 sediment cores (diameter = 10 cm) simultaneously. Four successful cores were selected from amongst the 12 cores for quantitative analysis of the benthic meiofauna. Nodules collected by a 0.25 m<sup>2</sup> box corer (Ocean Instruments BX-S50 MK-III) at the same stations during the cruise were used to estimate the nodule density of the area (Chuar et al., 2020). From the box core, a Shear Strength Measurement Tool (Humboldt H-4227) was also used to determine the shear strength of the sediment (Chuar et al., 2020), a measure of the stability of sediment (Grabowski, 2014). Shear strength readings were taken for 0–10 cm, 15–25 cm and 25–40 cm depths. The sampling location, date and depth of each station, as well as the shear strength reading for the 0–10 cm depth, and nodule data from 0–5 cm depth obtained from box corer deployments are listed in Table 2.

**Table 2.**

Stations in the OMS exploratory area during the research cruise ABYSSLINE 02 where the multiple corer was deployed. Shear strength (kPa) value for 0–10 cm sediment layer, surface nodule coverage (%), nodule weight (g) for 0–5 cm sediment layer, and nodule volume (cm<sup>3</sup>) for 0–5 cm sediment layer were based on box corer samples from the same location.

Station	Deployment ID	Date	Coordinates	Depth (m)	Shear strength (kPa)	Surface nodule coverage (%)	Nodule weight (g)	Nodule volume (cm <sup>3</sup> )
S01	MC07	24 Feb. 2015	12 07.07128 N 117 20.60474 W	4185	2.17	40.5	4219.47	2280
S02	MC10	28 Feb. 2015	12 04.90710 N 117 10.69599 W	4072	2.16	35.8	3228.07	1680
S03	MC08	25 Feb. 2015	12 10.86723 N 117 15.6556 W	4114	1.44	19.1	4527.64	2360
S04	MC09	27 Feb. 2015	12 00.563 N 117 10.690 N	4148	2.09	40.1	3671.63	1910
S05	MC11	1 Mar. 2015	12 13.036 N 117 19.520 W	4106	1.84	30.5	3346.23	1750
S06	MC12	2 Mar. 2015	12 08.695 N 117 19.527 W	4041	4.63	20.4	1759.34	920
S07	MC20	12 Mar. 2015	12 08.163 N 117 12.899 W	4110	1.94	33.2	4431	2210
S08	MC22	14 Mar. 2015	12 11.417 N 117 22.281 W	4179	0.63	0	45.02	15
S09	MC19	11 Mar. 2015	12 05.999 N 117 11.799 W	4082	2.34	35	3390.62	1805



S10	MC21	13 Mar. 2015	12 03.27253 N 117 15.09741 W	4096	2.00	42.8	4158.36	2050
S11	MC23	16 Mar. 2015	12 00.555 N 117 22.818 W	4152	2.25	23.8	3784.49	1975
S12	MC24	17 Mar. 2015	12 01.64107 N 117 19.51164 W	4127	2.81	38.5	6560.21	3680

173

174

175

176

177

178

179

180

181

182

183

184

185

186

187

188

189

190

191

192

193

194

195

196

197

198

199

200

201

202

203

204

205

206

207

208

209

210

211

212

213

214

215

216

217

218

219

220

221

222

223

224

225

226

227

228

229

### 2.3. Sample processing

On board the vessel, each intact sediment core was sliced into two layers: an upper 0–2 cm layer, and a lower 2–5 cm layer. Overlying water from each core was filtered through a 40  $\mu\text{m}$  mesh sieve and the filtrate added to the 0–2 cm layer. Each layer was then separately preserved in 10% borax-buffered formalin. In the laboratory of Senckenberg am Meer Wilhelmshaven, meiobenthic organisms were separated from the sediments using Levasil®-kaolin medium (McIntyre & Warwick, 1984) followed by three consecutive centrifugations at 4,000 g for 6 minutes each time. The centrifugal supernatant containing the organisms was then filtered through a 40  $\mu\text{m}$  mesh sieve, washed with fresh water, preserved in 10% borax-buffered formalin and stained with Rose Bengal. Sorting of the animals to their animal groups (i.e., major taxa including ‘Nauplii’) was done under Olympus SZH16 stereomicroscopes, using a Bogorov counting chamber, at the St John’s Island National Marine Laboratory, Singapore. The Nematoda was preserved in 10% borax-buffered formalin and the other animal groups were preserved in 70–80% ethanol for storage.

### 2.4. Data analysis

To examine differences among communities at the 12 stations, the abundance, richness (total number of animal groups) and diversity using Shannon-Wiener diversity indices were calculated. Meiofauna counts from the 0–5 cm sediment layer at each station were pooled from four cores, and then presented as the number of individuals (ind.) per 10  $\text{cm}^2$  prior to further analyses.

Spearman Rank correlation was used to elucidate the existence of possible relationships amongst environmental variables (i.e., shear strength, nodule cover, nodule weight, nodule volume) as determined from box core samples. Nodule weight and volume were not unexpectedly very significantly correlated ( $p\text{-value} < 0.01$ ,  $\rho = 0.99$ ) and thus nodule weight was excluded from further analyses. Overall, only three environmental parameters were used for analyses in this study: shear strength (kPa), nodule cover (%) and nodule volume ( $\text{cm}^3$ ). Spearman Rank correlation between abundance and diversity was also determined to find out their possible relationships with environmental parameters.

Multivariate analyses with abundance data were performed on fourth-root transformed, Bray-Curtis dissimilarity matrix, and environmental variables were untransformed and normalised. Cluster analyses with Type 1 Similarity Profile (SIMPROF) were used to test for any significant clusters. Non-metrical dimensional scaling (nMDS) was used to visualise any patterns in community composition across the 12 stations. BVStep (Spearman Rank correlation) was used to determine which animal groups best explained the differences among stations. BVStep could be considered a generalisation of Similarity Percentages (SIMPER) because the latter routine compares only two groups at a time (Clarke & Gorley, 2015). Marginal and sequential distance-based linear models (DISTLM) tests, visualised using distance-based redundancy analysis (dbRDA), were used to analyse any relationship between communities at the 12 stations in response to environmental variables. Within-group variability was tested using PERMANOVA and PERMDISP.

Spearman Rank correlation tests and Shannon-Wiener diversity indices were calculated using statistical software R version 3.6.1 (R Core Team, 2019). All multivariate tests were conducted in PRIMER v7 (Clarke & Gorley, 2015) with PERMANOVA+ add-on (Anderson et al., 2008). All analyses were carried out at 5% significance level.

### 3. RESULTS

#### 3.1. Abundance and diversity of metazoan meiofauna

Overall, 88 867 individuals were collected from 23 animal groups (including a group containing undetermined organisms, the 'Unknowns') across 13 phyla (Table 3; see also Appendix).

**Table 3.**

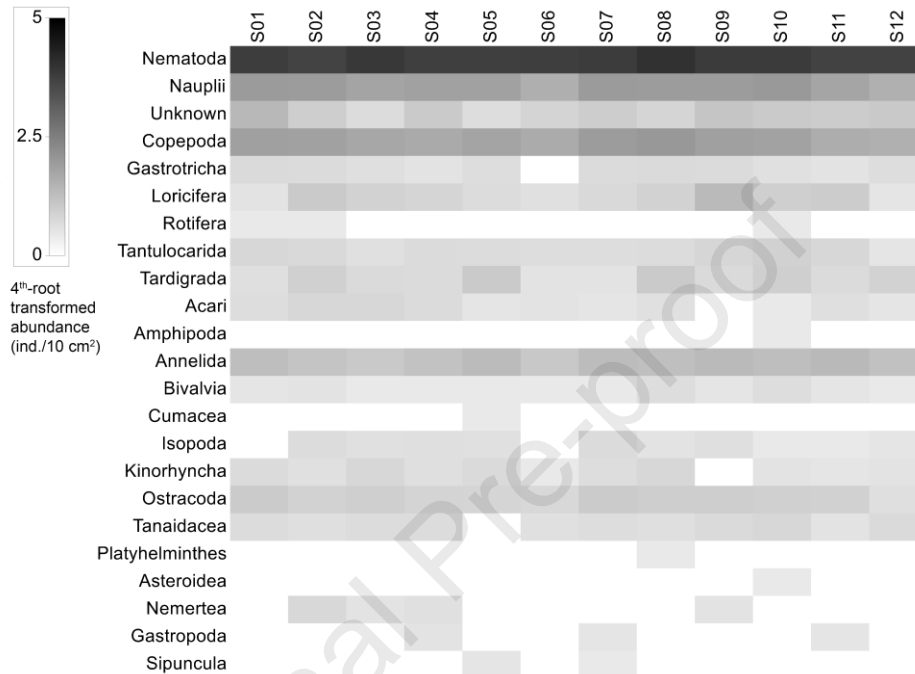
Abundance (ind./10 cm<sup>2</sup>) of metazoan meiofauna (animals retained on a 40 µm sieve) collected at each station in the OMS area of the CCFZ, eastern Pacific Ocean. Meiofauna counts from 0–5 cm sediment layer were pooled from four cores (diameter of each core = 10 cm) and then calculated to individuals/10 cm<sup>2</sup>. s.d. = standard deviation.

Animal groups/Station	1	2	3	4	5	6	7	8	9	10	11	12	Mean	s.d.
<b>Phylum Platyhelminthes</b>	0.00	0.00	0.00	0.00	0.00	0.00	0.00	0.03	0.00	0.00	0.00	0.00	0.00	0.01
<b>Phylum Nemertea</b>	0.00	0.35	0.10	0.13	0.00	0.00	0.00	0.00	0.10	0.00	0.00	0.00	0.06	0.10
<b>Phylum Nematoda</b>	207. 28	179. 94	227. 62	199. 48	198. 94	203. 34	208. 62	262. 54	213. 97	212. 73	186. 24	185. 54	207. 19	22.0 6
<b>Phylum Gastrotricha</b>	0.29	0.25	0.16	0.10	0.19	0.00	0.25	0.29	0.25	0.13	0.10	0.19	0.18	0.09
<b>Phylum Rotifera</b>	0.03	0.03	0.00	0.00	0.00	0.00	0.00	0.00	0.00	0.03	0.00	0.00	0.01	0.01
<b>Phylum Loricifera</b>	0.10	1.18	0.57	0.45	0.22	0.13	0.32	0.60	3.28	0.76	0.95	0.06	0.72	0.88
<b>Phylum Kinorhyncha</b>	0.25	0.13	0.38	0.16	0.29	0.03	0.19	0.38	0.00	0.10	0.06	0.10	0.17	0.13
<b>Phylum Annelida</b>														
Polychaeta	2.61	1.81	1.21	1.97	3.12	1.34	2.93	2.48	3.25	2.67	3.41	2.20	2.42	0.72
<b>Phylum Sipuncula</b>	0.00	0.00	0.00	0.00	0.06	0.00	0.03	0.00	0.00	0.00	0.00	0.00	0.01	0.02
<b>Phylum Tardigrada</b>	0.16	0.70	0.29	0.25	1.18	0.10	0.10	1.15	0.29	0.76	0.25	0.60	0.49	0.39
<b>Phylum Arthropoda</b>														
Acari	0.19	0.38	0.38	0.25	0.06	0.10	0.06	0.13	0.00	0.03	0.16	0.06	0.15	0.13
Amphipoda	0.00	0.00	0.00	0.00	0.00	0.00	0.00	0.00	0.00	0.03	0.00	0.00	0.00	0.01
Copepoda	11.7 8	11.4 9	8.69	7.67	10.1 9	7.19	14.2 6	16.3 3	11.8 7	10.8 5	6.72	5.63	10.2 2	3.19
Cumacea	0.00	0.00	0.00	0.00	0.03	0.00	0.00	0.00	0.00	0.00	0.00	0.00	0.00	0.01
Isopoda	0.00	0.22	0.13	0.16	0.13	0.00	0.25	0.10	0.16	0.03	0.03	0.06	0.11	0.08
Ostracoda	1.08	0.57	0.80	0.48	0.45	0.35	1.05	0.86	0.83	0.70	0.67	0.16	0.67	0.28
Tanaidacea	0.22	0.16	0.22	0.22	0.00	0.13	0.19	0.16	0.29	0.38	0.10	0.29	0.20	0.10
Tantulocarida	0.38	0.32	0.13	0.25	0.22	0.19	0.19	0.22	0.41	0.67	0.38	0.06	0.29	0.16
Nauplii	14.4 5	13.8 5	9.99	11.2 7	11.3 6	5.83	14.4 5	14.0 4	13.7 2	16.0 4	9.58	5.63	11.6 8	3.40
<b>Phylum Mollusca</b>														
Bivalvia	0.06	0.10	0.03	0.03	0.03	0.03	0.03	0.19	0.06	0.19	0.06	0.03	0.07	0.06
Gastropoda	0.00	0.00	0.00	0.10	0.00	0.00	0.06	0.00	0.00	0.00	0.06	0.00	0.02	0.03
<b>Phylum Echinodermata</b>														
Asteroidea	0.00	0.00	0.00	0.00	0.00	0.00	0.00	0.00	0.00	0.03	0.00	0.00	0.00	0.01
<b>Unknown</b>	3.63	0.86	0.22	1.15	0.19	0.48	0.92	0.45	1.66	1.11	1.02	1.24	1.08	0.92
<b>Total abundance (ind./10 cm<sup>2</sup>)</b>	242. 52	212. 34	250. 92	224. 12	226. 67	219. 22	243. 92	299. 94	250. 13	247. 26	209. 80	201. 87	235. 73	26.3 9
<b>Richness</b>	15	17	16	17	16	13	17	16	14	18	16	15	15.8 3	1.40
<b>Shannon-Wiener index</b>	0.63	0.66	0.45	0.52	0.55	0.36	0.61	0.55	0.65	0.61	0.53	0.41	0.54	0.10

The number of individuals ranged from 201.9 ind./10 cm<sup>2</sup> at Station 12 to 299.9 ind./10 cm<sup>2</sup> at Station 8 (Table 3). The average meiofaunal abundance across the 12 stations within the 30 × 30 km sampling area was 235.7 ± 26.4 ind./10 cm<sup>2</sup>

246 (Table 3). Despite the near absence of nodules at Station 8, diversity and abundance of meiofauna were among the  
 247 highest (Table 3).  
 248

249 Nematoda, Nauplii, Copepoda, Loricifera, Tantulocarida, Tardigrada, Annelida, Bivalvia, Ostracoda and Unknowns  
 250 were present at all 12 stations (Fig. 3). The Nematoda was the dominant animal group (mean of  $87.9 \pm 2.9\%$ ), followed  
 251 by the Nauplii ( $5.0 \pm 1.3\%$ ) and the Copepoda ( $4.3 \pm 1.1\%$ ). Other animal groups comprised the remaining 2.9% (Fig.  
 252 3; see Appendix). A few animal groups were only present in just one or two stations. Amphipoda was only present in  
 253 Station 10; Cumacea in Station 5; Platyhelminthes in Station 8; Asteroidea in Station 10; and Sipuncula in Stations 5  
 254 and 7 (Fig. 3).  
 255  
 256



257  
 258 **Fig. 3** Shade plot of the 4<sup>th</sup>-root transformed abundance (ind./10 cm<sup>2</sup>) data of each animal group at each of the 12 stations. Darker spaces indicated  
 259 higher abundances. White spaces indicate a total absence of the animal group.  
 260  
 261

262 Significant negative correlations were only found between meiofaunal abundances and shear strength (p-value = 0.02,  
 263 rho = -0.66) (Table 4). No significant correlations were found between diversity (based on the Shannon-Wiener Index)  
 264 and environmental parameters (Table 4).  
 265

266 **Table 4.**  
 267 Spearman rank correlations of abundance and Shannon-Wiener diversity indices with environmental variables.  
 268

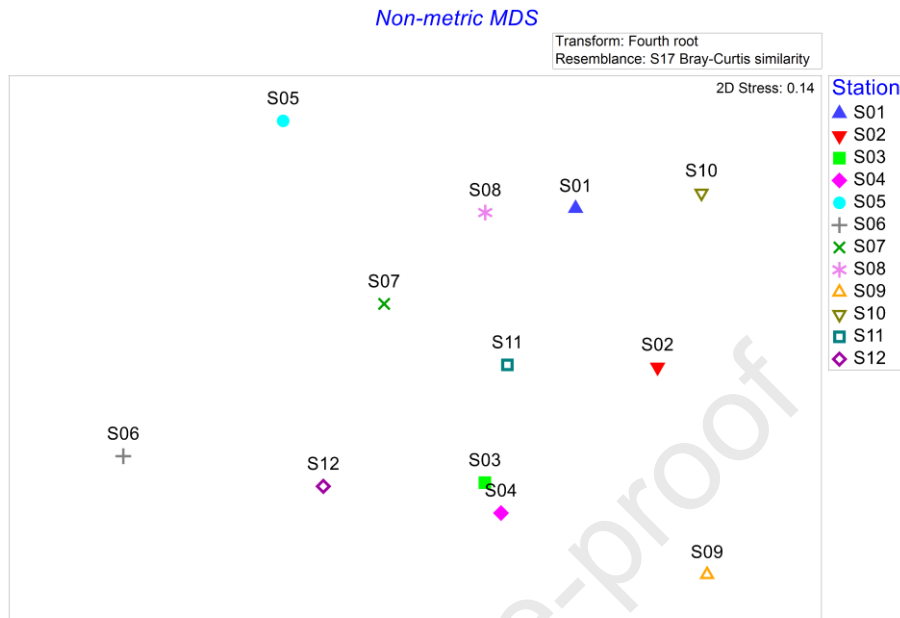
	Shear strength		Nodule cover		Nodule volume	
	rho	p-value	rho	p-value	rho	p-value
<b>Abundance</b>	-0.66	0.02	-0.26	0.42	-0.09	0.78
<b>Shannon-Wiener diversity index</b>	-0.16	0.62	0.35	0.27	-0.15	0.64

269  
 270

### 271 3.2. Multivariate analyses of community structure

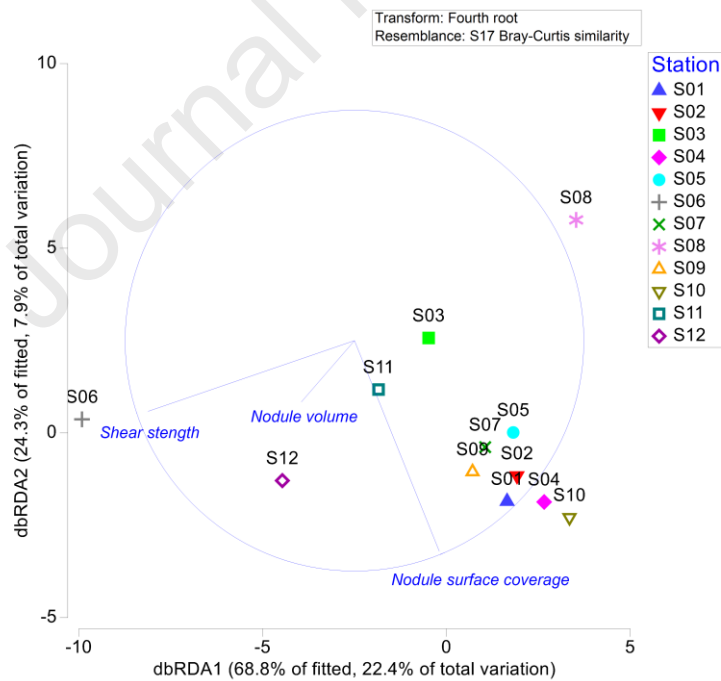
272  
 273 Based on the animal group composition and abundance, cluster analyses showed no clusters supported by SIMPROF.  
 274 Similarly, from the nMDS (Fig. 4), there was also no obvious groupings across the 12 stations. BVStep selected a high  
 275 number of 13 animal groups—Nauplii, Copepoda, Gastrotricha, Loricifera, Rotifera, Tardigrada, Amphipoda, Bivalvia,  
 276 Cumacea, Kinorhyncha, Nemertea, Sipuncula and Unknown, that best explain the variability among stations  
 277 contributing to the overall multivariate pattern. From the BVStep procedure, the differences among stations were driven  
 278 by the less abundant animal groups. This number was also more than half of the total number of 23 identified animal  
 279 groups. This might also suggest that OMS area is very diverse since so many animal groups contributed to the  
 280 multivariate pattern. DISTLM results indicated that both nodule surface coverage and nodule volume (both marginal  
 281 and sequential p-values < 0.05) did not explain the meiofaunal community variation at the major taxon level, and only  
 282 results for sediment shear strength was significant (marginal test p-value = 0.03, R<sup>2</sup> = 0.18, Pseudo-F = 2.21; sequential  
 283 tests mostly significant, or p-values very close to 0.05) (Fig. 5). This could also indicate that there are other factors

284 explaining the variation in meiofaunal community, which should be measured in future expeditions. Within each  
 285 station, high average similarity of >80 was observed among the four cores for both relative and absolute abundances  
 286 (Appendix), and PERMDISP did not show any significance ( $p(\text{perm}) = 0.41$  and  $p(\text{perm}) = 0.75$  respectively).  
 287 PERMANOVA (Pseudo-F = 2.27,  $P(\text{perm}) = < 0.01$ ) and pair-wise comparisons showed that almost all the stations  
 288 were different from each other (Appendix).  
 289



290  
 291  
 292

**Fig. 4.** Non-metric dimensional scaling (nMDS) visualisation of the 12 stations (0–5 cm sediment layer) in the OMS area of the CCFZ.



293  
 294  
 295  
 296  
 297  
 298  
 299  
 300  
 301  
 302  
 303

**Fig. 5.** Distance-based redundancy analysis (dbRDA) illustrating the DISTLM based on meiofaunal community data (0–5 cm sediment layer) and environmental data. The length and direction of vectors represent the strength and direction of the relationship.

## 304 3.3. Vertical distribution

305  
306 Across all animal groups, the majority (76.6%) of the animals were found in the top 0–2 cm sediment layer (Table 5).  
307

308 **Table 5.**  
309 Percentage (%) of each animal group in the 0–2 cm and 2–5 cm sediment layers, arranged in descending quantities. s.d. = standard deviation.  
310

Sediment layer Station	0–2 cm												Mean	s.d.
	1	2	3	4	5	6	7	8	9	10	11	12		
Nematoda	72.86	57.05	60.04	70.59	72.18	69.00	65.29	53.42	69.03	71.37	73.66	61.61	66.34	6.77
Nauplii	5.50	5.70	2.98	4.57	4.72	2.24	5.19	4.01	4.98	5.97	3.99	2.05	4.32	1.31
Copepoda	4.37	4.71	2.65	2.85	3.93	2.58	4.95	4.61	4.12	4.00	2.73	1.94	3.62	1.01
Annelida	1.00	0.72	0.34	0.81	1.32	0.54	1.11	0.65	1.20	1.02	1.38	0.85	0.91	0.32
Ostracoda	0.41	0.25	0.24	0.18	0.20	0.16	0.39	0.23	0.17	0.28	0.30	0.05	0.24	0.10
Loricifera	0.04	0.06	0.05	0.18	0.08	0.03	0.09	0.05	0.81	0.28	0.39	0.03	0.18	0.23
Tardigrada	0.05	0.24	0.05	0.10	0.51	0.04	0.03	0.22	0.11	0.31	0.12	0.24	0.17	0.14
Tantularcarida	0.13	0.13	0.04	0.10	0.10	0.09	0.05	0.07	0.15	0.26	0.15	0.02	0.11	0.06
Gastrotricha	0.09	0.10	0.06	0.04	0.08	0.00	0.10	0.07	0.09	0.05	0.05	0.05	0.07	0.03
Kinorhyncha	0.11	0.06	0.13	0.06	0.13	0.01	0.08	0.11	0.00	0.04	0.03	0.05	0.07	0.04
Tanaidacea	0.09	0.06	0.08	0.07	0.00	0.06	0.07	0.04	0.11	0.15	0.05	0.06	0.07	0.04
Acari	0.05	0.13	0.15	0.10	0.03	0.03	0.01	0.04	0.00	0.01	0.08	0.02	0.05	0.05
Bivalvia	0.03	0.03	0.01	0.01	0.01	0.01	0.01	0.06	0.01	0.06	0.03	0.02	0.03	0.02
Isopoda	0.00	0.04	0.04	0.06	0.06	0.00	0.08	0.02	0.05	0.01	0.00	0.02	0.03	0.03
Nemertea	0.00	0.16	0.04	0.06	0.00	0.00	0.00	0.00	0.04	0.00	0.00	0.00	0.02	0.05
Gastropoda	0.00	0.00	0.00	0.04	0.00	0.00	0.03	0.00	0.00	0.00	0.03	0.00	0.01	0.02
Amphipoda	0.00	0.00	0.00	0.00	0.00	0.00	0.00	0.00	0.00	0.01	0.00	0.00	0.00	0.00
Asteroidea	0.00	0.00	0.00	0.00	0.00	0.00	0.00	0.00	0.00	0.01	0.00	0.00	0.00	0.00
Cumacea	0.00	0.00	0.00	0.00	0.01	0.00	0.00	0.00	0.00	0.00	0.00	0.00	0.00	0.00
Platyhelminthes	0.00	0.00	0.00	0.00	0.00	0.00	0.00	0.01	0.00	0.00	0.00	0.00	0.00	0.00
Rotifera	0.00	0.00	0.00	0.00	0.00	0.00	0.00	0.00	0.00	0.01	0.00	0.00	0.00	0.00
Sipuncula	0.00	0.00	0.00	0.00	0.03	0.00	0.01	0.00	0.00	0.00	0.00	0.00	0.00	0.01
Unknown	1.44	0.12	0.05	0.48	0.06	0.20	0.29	0.08	0.55	0.30	0.15	0.50	0.35	0.39
<b>Percentage of meiofauna in the 0– 2 cm sediment layer</b>	86.17	69.58	66.95	80.32	83.44	75.00	77.78	63.72	81.42	84.17	83.14	67.49	76.60	7.81
Sediment layer Station	2–5 cm												Mean	s.d.
	1	2	3	4	5	6	7	8	9	10	11	12		
Nematoda	12.61	27.69	30.67	18.42	15.59	23.75	20.24	34.11	16.52	14.66	15.11	30.31	21.64	7.39
Nauplii	0.46	0.82	1.00	0.45	0.29	0.42	0.73	0.67	0.51	0.51	0.58	0.74	0.60	0.20
Copepoda	0.49	0.70	0.81	0.57	0.56	0.70	0.90	0.84	0.62	0.39	0.47	0.85	0.66	0.17
Annelida	0.08	0.13	0.14	0.07	0.06	0.07	0.09	0.18	0.10	0.06	0.24	0.24	0.12	0.07
Ostracoda	0.04	0.01	0.08	0.03	0.00	0.00	0.04	0.05	0.17	0.00	0.02	0.03	0.04	0.05
Loricifera	0.00	0.49	0.18	0.01	0.01	0.03	0.04	0.15	0.50	0.03	0.06	0.00	0.13	0.18
Tardigrada	0.01	0.09	0.06	0.01	0.01	0.00	0.01	0.16	0.00	0.00	0.00	0.06	0.04	0.05
Tantularcarida	0.03	0.01	0.01	0.01	0.00	0.00	0.03	0.00	0.01	0.01	0.03	0.02	0.01	0.01
Gastrotricha	0.03	0.01	0.00	0.00	0.00	0.00	0.00	0.02	0.01	0.00	0.00	0.05	0.01	0.02
Kinorhyncha	0.00	0.00	0.03	0.01	0.00	0.00	0.00	0.02	0.00	0.00	0.00	0.00	0.01	0.01
Tanaidacea	0.00	0.01	0.01	0.03	0.00	0.00	0.01	0.01	0.00	0.00	0.00	0.08	0.01	0.02
Acari	0.03	0.04	0.00	0.01	0.00	0.01	0.01	0.00	0.00	0.00	0.00	0.02	0.01	0.01
Bivalvia	0.00	0.01	0.00	0.00	0.00	0.00	0.00	0.00	0.01	0.01	0.00	0.00	0.00	0.01
Isopoda	0.00	0.06	0.01	0.01	0.00	0.00	0.03	0.01	0.01	0.00	0.02	0.02	0.01	0.02
Nemertea	0.00	0.00	0.00	0.00	0.00	0.00	0.00	0.00	0.00	0.00	0.00	0.00	0.00	0.00
Gastropoda	0.00	0.00	0.00	0.00	0.00	0.00	0.00	0.00	0.00	0.00	0.00	0.00	0.00	0.00
Amphipoda	0.00	0.00	0.00	0.00	0.00	0.00	0.00	0.00	0.00	0.00	0.00	0.00	0.00	0.00
Asteroidea	0.00	0.00	0.00	0.00	0.00	0.00	0.00	0.00	0.00	0.00	0.00	0.00	0.00	0.00
Cumacea	0.00	0.00	0.00	0.00	0.00	0.00	0.00	0.00	0.00	0.00	0.00	0.00	0.00	0.00
Platyhelminthes	0.00	0.00	0.00	0.00	0.00	0.00	0.00	0.00	0.00	0.00	0.00	0.00	0.00	0.00
Rotifera	0.01	0.01	0.00	0.00	0.00	0.00	0.00	0.00	0.00	0.00	0.00	0.00	0.00	0.01
Sipuncula	0.00	0.00	0.00	0.00	0.00	0.00	0.00	0.00	0.00	0.00	0.00	0.00	0.00	0.00
Unknown	0.05	0.28	0.04	0.03	0.03	0.01	0.09	0.06	0.11	0.15	0.33	0.11	0.11	0.10
<b>Percentage of meiofauna in the 2– 5 cm sediment layer</b>	13.83	30.42	33.05	19.68	16.56	25.00	22.22	36.28	18.58	15.83	16.86	32.51	23.40	7.81

311  
312  
313  
314

315 **4. DISCUSSION**

316  
317 *4.1 Meiofaunal abundance, diversity and community structure across the CCFZ*

318  
319 In this study, our comparatively small sampling area of  $30 \times 30$  km is only ~1.5% of the total allocated OMS area  
320 (58,280 square kilometers). Yet, even at the level of major taxonomic groups, our results based on multivariate analyses  
321 suggested that the meiofaunal community structure at each of the 12 stations is different, demonstrating that the eastern  
322 region of the CCFZ sea floor is very diverse. The average of  $235.7 \pm 26.4$  ind./10 cm<sup>2</sup> across the 12 stations was also  
323 relatively higher than previously reported meiofaunal abundances in the other CCFZ areas (Table 6, Fig. 6). There were  
324 some exceptions in a few stations across the various studies where more meiobenthos were found (values in bold font in  
325 Table 6). At the eastern end, the BGR contract area ( $483.8 \pm 95.2$  ind./10 cm<sup>2</sup>,  $371.8 \pm 33.1$  ind./10 cm<sup>2</sup> and  $306.6 \pm$   
326  $99.0$  ind./10 cm<sup>2</sup>) (Hauquier et al., 2019; Uhlenkott et al., 2020), the IOM contract area ( $244.6$ – $394.2$  ind./10 cm<sup>2</sup>,  $552.7$   
327  $\pm 260.3$  ind./10 cm<sup>2</sup>) (Radziejewska, 2002; Hauquier et al., 2019), and the GSR contract area at B6S02April ( $242.3 \pm$   
328  $59.2$  ind./10 cm<sup>2</sup>) (Pape et al., 2017) found higher meiofaunal abundance compared against our 0–5 cm layer results.  
329 The NIXO 47 study reported meiofaunal abundance of 187–247 ind./10 cm<sup>2</sup> from some box corer samples (0–2.5 cm  
330 sediment depth), which was also comparable to our results from the 0–2 cm layer (Renaud-Mornant & Gourbault,  
331 1990). The KODOS studies utilized sediment layers up to 3 cm depth and found 181 ind./10 cm<sup>2</sup>, 229 ind./10 cm<sup>2</sup>, 222  
332 ind./10 cm<sup>2</sup> at W135, M03 and M04 respectively (Kim et al., 2004; Min et al., 2018), which were comparable to our 0–  
333 2 cm and 0–5 cm findings.

334  
335 Results from NIXO 47, DOMES, ECHO-1, PRA, IOM-BIE, and JET expeditions, as well as those from survey cruises  
336 in GSR, KODOS and COMRA exploration sites (see Fig. 6; Table 6 and references therein) have provided some of the  
337 first meiofaunal abundance and composition data from the CCFZ. Differences in collection methods (e.g., multiple  
338 corer or subsamples from box corer), lower sieve size limits, and sediment depths sampled make direct comparisons  
339 difficult across these studies. However, it is also not possible to exclude all studies using different collection methods or  
340 sieve sizes due to the already very limited data from the CCFZ. Hence, to maintain meaningful comparisons, we  
341 retained studies using lower sieve size limits of maximum 63  $\mu$ m, and at similar CCFZ depths of around 4000–5000 m  
342 (Table 6). Any comparisons made were as far as possible within the same sediment layer, or across similar sediment  
343 layers. The DOMES study (Hecker & Paul, 1979) and PRA sites (Wilson, 1990, 1992) only included meiofaunal groups  
344 sized >300  $\mu$ m and were therefore excluded from comparisons here.  
345

346  
347  
348  
349**Table 6.**

Expedition information and meiofaunal abundances from various studies in the CCFZ. Abundances in bold indicate higher meiofaunal abundances relative to this study. Data from sediment depths of 0–2 cm and 0–5 cm of this study were included to facilitate comparisons. s.d. = standard deviation.

Name of expedition	Contractor/Contract area in CCFZ	Year of expedition	Depth (m)	Sampling method	Lowest sieve size ( $\mu\text{m}$ )	Sampling depth (cm)	No. or name of stations	No. or name of replicates	Abundance $\pm$ s.d. (ind./10 $\text{cm}^2$ )	Remarks	Reference		
ABYSSLINE 02	Ocean Mineral Singapore (Singapore)	2015	4000–4200	Multiple corer	40	0–5	12		235.73 $\pm$ 26.39		This study		
						0–2			180.13 $\pm$ 23.09				
Mangan2010,2013,2014,2016,2018, EcoResponse	BGR (Germany)	2010, 2013, 2014, 2015, 2016, 2018	4076–4156	Multiple corer	32	0–5	35 deployments, 106 cores		<b>306.62 <math>\pm</math> 98.95</b>	converted from 100 $\text{cm}^2$ to 10 $\text{cm}^2$ , summed the meiofaunal abundance from each core, and then averaged it by the total number of cores BGR area divided into “Reference area” (BGR_RA; limited future mining) and “Prospective area” (BGR_PA; intensive future mining)	Uhlenkott et al., 2020		
			4342.2						BGR_PA			5 deployments	<b>371.84 <math>\pm</math> 33.11</b>
			4123.9						BGR_RA			5 deployments	<b>483.84 <math>\pm</math> 95.18</b>
SQ239	IOM (Interoceanmetal Joint Organization)	2015	4434.5	Multiple corer	32	0–5	3	3 deployments	<b>552.71 <math>\pm</math> 260.32</b>		Martínez Arbizu & Haeckel, 2015; Hauquier et al., 2019		
			4839.1					APEI-3	4 deployments			53.20 $\pm$ 8.86	
			4964.6					IFREMÉR (France)	5 deployments			182.15 $\pm$ 62.42	
			4511.8					DEME-GSR (Belgium)	5 deployments			211.49 $\pm$ 40.36	
IOM-BIE	IOM (Interoceanmetal Joint Organization)	1995	4380–4430	Multiple corer	32	0–6		MC1	100.66		Radziejewska, 2002		
								MC2	105.70				
								MC3	<b>245.14</b>				
								MC4	86.10				
								MC5	<b>277.76</b>				
								MC6	<b>394.24</b>				
		1997	MO1	<b>244.56</b>	control (C2)								
			MO2	198.94	control (C2)								

									MO3	152.88	control (C2)	
		4380–4410							3 cores	91.56 ± 23.31	nodule bearing area; abundance data taken from Radziejewska (2014)	Radziejewska & Modlitba, 1999; Radziejewska, 2014
		4412–4436							3 (MO2, MO22, MO23)	138.97 ± 3.49	control only (C3)	Radziejewska et al., 2001
SO239		4522–4526							B6S02 April 4	<b>242.3 ± 59.2</b>		
		4470–4526							B6S02 Oct 3	151.1 ± 54.2		Pape et al., 2017
GSRNOD15A									B4S03 3	106.6 ± 29.3		
									B4N01 3	88.1 ± 55.0		
	GSR (Belgium)		Multiple corer	32	0–5				NodFree (B4S03) 4	126.8 ± 29.0		
GSRNOD17		4480–4649							NodRich_A (B4S03) 4	87.0 ± 21.0		Pape et al., 2021
									NodRich_B (B4S03) 3	45.4 ± 31.5		
									H347	92.98		
									H349	160.53		
									H350	30.53	used only the controls at 0–1 cm layer; modified original data to exclude the Foraminifera, Protozoa and Calanoida	
ECHO-1		4480–4517	Box corer	63	0–1				H351	98.25		Wilson & Hessler, 1987
									H352	8.77		
									H360	118.42		
									H362	31.58		
									Baseline studies from five box cores, two subcores taken from each box core samples	46.2–205.3		
NOAA-BIE	US-Russian Joint BIE in a test site in Russian contract area	4800	Box corer	45	0–3						total meiobenthos abundance data taken from Radziejewska (2014)	Trueblood & Ozturgut, 1997; Trueblood et al., 1997; Radziejewska, 2014
									Five control multicorer samples	40.74–91.28		
		5035–5042							Five stations sampled, total of eight corers	181.66 ± 35.56	outside nodule area	
NODINAUT	IFREMER (France)	4877–5000	Multiple corer		0–5				Five stations sampled, total of eight corers	95.97 ± 23.43	nodule area	Mahatma, 2009
									47001 A	<b>189</b>		
									47004 A,B	124		
NIXO 47		4905–5140	Box corer	40	0–2.5				47007 A,B	134	modified original data by adding subsamples A,B from the same box corer together	Renaud-Mornant & Gorbault, 1990
									47011 A,B	110		
									47012 A,B	124		



						47014	A,B	<b>247</b>			
						47016	A,B	103			
						47018	A,B	156			
						47021	A,B	<b>187</b>			
						47024	A,B	120			
						47026	A,B	<b>203</b>			
						47029	A,B	<b>208</b>			
						47031	A,B	<b>187</b>			
						47032	A,B	149			
						47034	A,B	<b>220</b>			
						47036	A,B	95			
						47037	A,B	164			
						N05		102.50			
						N06		101.75			
						N07		123.50	averaged; modified original data to exclude the Foraminifera	Kim et al., 2000; Min et al., 2004; Min et al., 2018	
					N08		75.00				
					N09		72.75				
					N10		90.75				
						N12		67			
						N13		54			
						N14		4		Min et al., 2004; Min et al., 2018	
						N16		6			
						N17		27			
"KODOS"	Korea Deep Ocean Study area (Korea)	1998, 1999, 2001, 2003, 2004, 2005	4090–5091	Multiple corer	37–63	upper 3 cm	W128		84		
							W129		61		
							W130		83	modified original data to exclude the Foraminifera	
							W131		69		
							W131-1		91		
							W131-2		66		Min et al., 2018
							W132		97		
							W133		66		
							W134		50		
							W135		<b>181</b>		
							W136		119		
							M01		95		

									M02	38		
									M03	<b>229</b>		
									M04	<b>222</b>	modified original data to exclude the Foraminifera	Kim et al., 2004; Min et al., 2018
									M05	53		
									M06	71		
									M07	44		
JET1 (Japan Deep-sea Impact Experiment)	Japanese contract area	1994 (prior to disturbance )	~5300	Multiple corer	30	0-3	10	44 subcores		101.0 ± 55.9	meiofauna from 30-300 µm	Kaneko et al., 1997
	China Ocean Mineral Resources Research and Development Association (COMRA) EAST	2005	5100- 5400		38	0-1,1- 2,2-4,4- 6	6			104.40 ± 20.48		Wang et al., 2013
"COMRA"		1998	~5000- 5300	Multiple corer	32	0-1,1- 2,2-4,4- 6	10			32.47	average	Gao et al., 2002
	China Ocean Mineral Resources Research and Development Association (COMRA) WEST	2005	5100- 5400		38	0-1,1- 2,2-4,4- 6	6			40.26 ± 25.84		Wang et al., 2013
		1998	~5000- 5300		32	0-1,1- 2,2-4,4- 6	10			18.05	average	Gao et al., 2002
	Polymetallic Nodule Field	2013	5193	1 random core taken using a perspex tube	31	0-1,1- 2,2-4,4- 6,6-8	WS1303			45.30		Zhao et al., 2020
			5133				PRZ1302			4.97		

350  
351  
352  
353

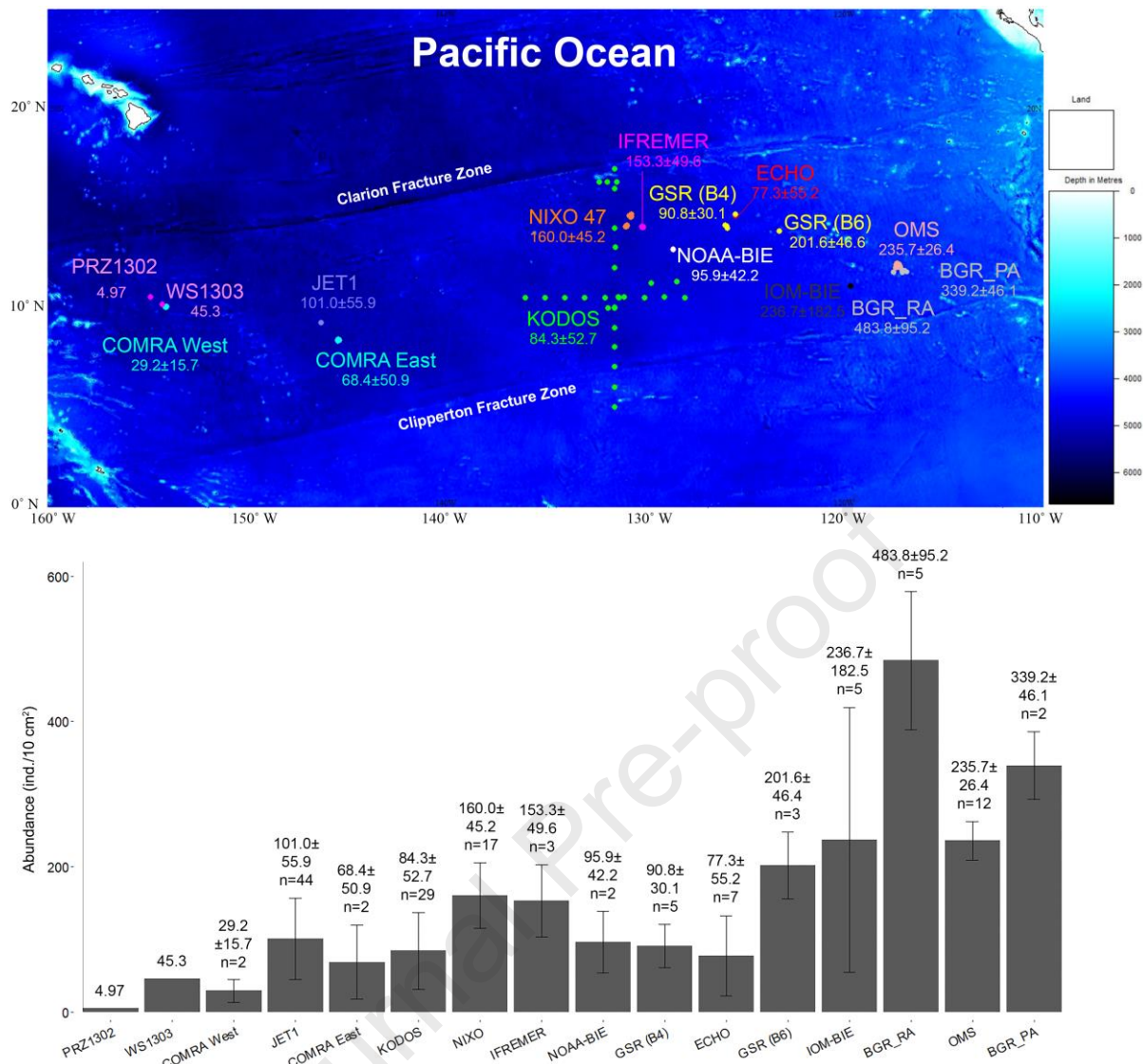


**Fig. 6.** Mean meiofaunal abundances (ind./10 cm<sup>2</sup>) ± s.d. in the CCFZ obtained from various expeditions (see Table 6 for details). The coloured points represent locations of sampling stations. Stations PRZ1302 and WS1303 (closer to COMRA West) were from Zhao et al. (2020). For the GSR contract area, GSR (B4) is further to the west and GSR (B6) is further to the east. The BGR contract area was divided into BGR\_RA and BGR\_PA (east of OMS sampling locations in this study). Sampling locations from Uhlenkott et al. (2020) were east of OMS, and were therefore combined with data from BGR\_PA. The means for COMRA West, COMRA East, IFREMER, GSR (B4), GSR (B6) and BGR\_PA were calculated from the means obtained from the various studies (refer to Table 6). The IOM-BIE value was calculated using data from Hauquier et al. (2019), Radziejewska (2014), and the means obtained from C1, C2 and C3 (Radziejewska et al., 2001; Radziejewska, 2002, 2014). The value for NOAA-BIE was obtained by averaging the means of the min and max values reported in Radziejewska (2014). Breakdown of the calculations used in the bar chart can also be found in the Appendix. Map based on GEBCO (General Bathymetric Chart of the Oceans) Digital Atlas published by the British Oceanographic Data Centre on behalf of IOC and IHO, 2003. s.d. = standard deviation.

Regardless, similar to the macrofauna (Veillette et al., 2007b; Wilson, 2017; Chuar et al., 2020), a trend of decreasing meiofaunal abundance from east to west across the CCFZ can be observed (Fig. 6 and Table 6). The upwelling of nutrient rich waters along the equator, as well as the presence of eddies and easterly trade winds contribute to more intense sea surface productivity in the eastern end of the CCFZ, which gradually decreases westwards (Smith & Demopoulous, 2003; Hannides & Smith, 2003). Faunal abundance and diversity could be influenced by this westward reduction of sea surface productivity and therefore a decrease of particulate organic carbon (POC) flux across the CCFZ (Smith & Demopoulous, 2003; Hannides & Smith, 2003; De Smet et al., 2017; Christodoulou et al., 2020; Laroche et al., 2020; Nomaki et al., 2021; Washburn et al., 2021). As deep-sea environments are usually food limited, POC flux, on a regional scale, plays a significant role in determining biological community structure on the sea floor (Smith et al., 1997, 2008; Bonifácio et al., 2020).

Similar to other studies in the CCFZ (Wilson & Hessler, 1987; Kaneko et al., 1997; Radziejewska & Modlitba, 1999; Kim et al., 2000; Gao et al., 2002; Min et al., 2004; Kim et al., 2004; Wang et al., 2013; Min et al., 2018), elsewhere in the Pacific Ocean (e.g., Snider et al., 1984; Shirayama, 1984) and other oceans worldwide (e.g., Ansari & Parulekar, 1981; Woods & Tietjen, 1985; Shirayama & Kojima, 1994; Zeng et al., 2018), the majority of meiobenthos are concentrated in the top sediment layers. Meiofaunal higher taxon composition (including “Nauplii”) was also similar, in

383 that the Nematoda was the most prevalent, or Foraminifera if the study included the protozoans, followed by the Nauplii  
 384 and Copepoda (Wilson & Hessler, 1987; Kaneko et al., 1997; Radziejewska et al., 2001; Kim et al., 2000; Gao et al.,  
 385 2002; Kim et al., 2004; Min et al., 2004; Wang et al., 2013; Pape et al., 2017; Min et al., 2018; Hauquier et al., 2019).

#### 387 *4.2 Sediment shear strength contributed to differences in meiofaunal communities and is negatively and significantly* 388 *correlated to meiofaunal abundance*

389 A significant negative correlation was apparent between sediment shear strength and meiofaunal abundance (i.e.,  
 390 meiofaunal abundance increase with decreasing shear strength), similar to the findings by Radziejewska & Modlitba  
 391 (1999). Sediment shear strength was also the only significant factor out of the three environmental parameters in this  
 392 study that contributed to the difference in meiofaunal community structure. The sediment shear strength may be  
 393 influenced by the size and gradation of individual particles (Langfelder & Nivargikar, 1967). It is commonly known  
 394 that coarser sediment and a larger grain size will result in an overall looser and less compact sediment (i.e., lower shear  
 395 strength value) (Trask & Rolston, 1950). Such conditions might provide habitat heterogeneity by increasing the number  
 396 of available microhabitats, which in turn result in higher diversity and abundance. Some studies did not find any  
 397 significant relationships between the meiofaunal community and granulometry (Hauquier et al., 2019; Pape et al.,  
 398 2021). Besides the intrinsic nature of the sediment, movements that occur naturally (e.g., by organisms, currents) could  
 399 affect shear strength as well (Richards & Parks, 1976). In a stable environment like the deep sea floor, bioturbation  
 400 caused by the movement of benthic animals could be one such biological process (Richards & Parks, 1976). The  
 401 differences in shear strength have previously been attributed to bioturbation because burrowing activities loosen  
 402 sediment and create chambers in the sediment, resulting in a lower shear strength value (Meadows et al., 1994;  
 403 Richardson et al., 1985). At the same time, more oxygen is made available to deeper layers, which could influence  
 404 benthic community structure (Aller & Aller, 1992; Löhr & Kennedy, 2015; Schratzberger & Ingels, 2018). These  
 405 factors might contribute to the differences in the meiofaunal abundance and community structure across the 12 stations.  
 406

#### 407 *4.3 Nodule parameters did not affect meiofaunal community structure at the major taxon level*

408 Based on the meiofaunal community at the major taxon level, there appeared to be no significant relationship with  
 409 nodules, suggesting that the meiofaunal community is not structured by these hard substratum habitats. Although the  
 410 crevices of the nodules can serve as microhabitats for the smaller metazoans (Thiel et al., 1993; Veillette et al., 2007b;  
 411 Pape et al., 2021), their abundances were much lower when compared to those found in the surrounding sediment (Thiel  
 412 et al., 1993). Some nematode genera or species were more abundant inside the nodules, indicating that metazoan  
 413 crevice fauna might be distinct from the adjacent sediment fauna (Thiel et al., 1993; Pape et al., 2021). However, while  
 414 Vanreusel et al. (2010) found that dominant Nematoda groups differed between areas with and without nodules in terms  
 415 of their locomotory behaviour, Pape et al. (2021) found that at least at the genus-level, no genera were endemic to the  
 416 nodule crevices.  
 417

418 Even so, we cannot discount the importance of these nodules for deep-sea fauna. In the CCFZ, 51% of all fauna are  
 419 facultatively or obligatorily associated with the nodules (Stratmann et al., 2021). A variety of organisms live on the  
 420 surface of the nodules, most of which are sessile taxa such as the Porifera, xenophyophores and other Foraminifera  
 421 (Dugolinsky et al., 1977; Veillette et al., 2007a, b; Vanreusel et al., 2016; Gooday et al., 2015, 2017a, b, 2018a, b; Lim  
 422 et al., 2017). These hard-substrate taxa would likely be distinct in their abundance and diversity from the sediment-  
 423 dwelling taxa (Dugolinsky et al., 1977; Mullineaux, 1987; Veillette et al., 2007a, b). Furthermore, these polymetallic  
 424 nodules are essential to maintain trophic and non-trophic interactions in the abyssal food-web and their removal will  
 425 result in knock-down effects on food-web integrity (Stratmann et al., 2021). Naturally, it is expected that the presence  
 426 or absence, and quantity of nodules will change the overall species composition of the benthic fauna. We also  
 427 emphasize here that our findings do not suggest that nodule removal during mining is not harmful towards the  
 428 meiofauna. Removal of surface sediment associated with the mining process directly kills the sediment fauna, and the  
 429 release of sediment and their redeposition will likely smother the seafloor community (Thiel et al., 2001).  
 430

## 431 **5. CONCLUSIONS**

432 Quantitative baseline data on the meiofaunal abundance and composition of the OMS contract area in the eastern region  
 433 of the CCFZ are provided for the first time. The CCFZ deep sea floor is very diverse, and community structure was  
 434 different between the stations, driven by the less abundant animal groups and sediment shear strength. Nodule surface  
 435 cover and nodule volume have no clear relationship with the meiofaunal community structure. The results of this study  
 436 also confirmed the westward decrease in meiofaunal abundance across the CCFZ. Although this current study focused  
 437 more on the sediment shear strength and the amount of nodules, additional environmental data (e.g., organic content,  
 438 bioturbation tests, sediment granulometry) could provide further insights in explaining differences in community  
 439 structure.  
 440

445 **FUNDING**

446 This work was supported by the Keppel-NUS Corporate Laboratory [grant number R-261-507-020-281].

447  
448 **DECLARATION OF COMPETING INTERESTS**

449 The authors declare that they have no known competing financial interests or personal relationships that could have  
450 appeared to influence the work reported in this paper.

451  
452 **SUBMISSION DECLARATION**

453 This article has not been published previously and is not currently under consideration for publication elsewhere.

454  
455 **ACKNOWLEDGEMENTS**

456  
457 The authors gratefully acknowledge the efforts of Professor Craig Smith, who led the UKSRL and OMS teams during  
458 ABYSSLINE 02, and his team from the University of Hawai'i, Manoa; Dr Pedro Martínez Arbizu and his team at the  
459 laboratory of Senckenberg am Meer Wilhelmshaven; all researchers and crew of R/V Thompson, National Research  
460 Foundation Singapore (NRF), Ocean Mineral Singapore and Keppel Corporation, UK Seabed Resources Limited, and  
461 the National University of Singapore for the success of the AB02 cruise. Bin Qi Gan thanks Dr Pedro Martínez Arbizu  
462 and his team for their training and guidance at the laboratory of Senckenberg am Meer Wilhelmshaven. We are also  
463 grateful to Lee Yen-Ling for her advice in statistical analyses; Lena Albers, Jutta Heitfeld and Marco Bruhn for their  
464 help and advice; Cheah Hoay Chuar for sorting the meiofauna and identifying the annelids; Rene Ong, Adrelia Teo and  
465 all volunteers for helping to sort the meiofauna. We also thank our anonymous reviewers for their constructive  
466 comments to improve the manuscript. The authors would like to acknowledge the St. John's Island National Marine  
467 Laboratory for providing the facility necessary for conducting the research. The Laboratory is a National Research  
468 Infrastructure under the National Research Foundation (NRF), Singapore. The authors are also grateful to the NRF,  
469 Keppel Corporation and National University of Singapore for supporting this work done in the Keppel-NUS Corporate  
470 Laboratory. The conclusions put forward reflect the views of the authors alone, and not necessarily those of the  
471 institutions within the Corporate Laboratory.

472  
473 **REFERENCES**

- 474  
475 Aller RC & Aller JY (1992) Meiofauna and solute transport in marine muds. *Limnology and Oceanography*, 37(5):  
476 1018–1033. DOI: <https://doi.org/10.4319/lo.1992.37.5.1018>
- 477  
478 Allsopp M, Miller C, Atkins R, Rocliffe S, Tabor I, Santillo D & Johnston P (2013) Review of the current state of  
479 development and the potential for environmental impacts of seabed mining operations. Greenpeace Research  
480 Laboratories Technical Report, 50 pp.
- 481  
482 Amon DJ, Hilario A, Martínez Arbizu P & Smith CR (2017) Observations of organic falls from the abyssal Clarion-  
483 Clipperton Zone in the tropical eastern Pacific Ocean. *Marine Biodiversity*, 47: 311–321. DOI:  
484 <https://doi.org/10.1007/s12526-016-0572-4>
- 485  
486 Anderson, MJ, Gorley RN & Clarke KR (2008). PERMANOVA+ for PRIMER: Guide for software and statistical  
487 methods. Plymouth: Primer-E Ltd, United Kingdom, 214 pp.
- 488  
489 Ansari ZA & Parulekar AH (1981) Meiofauna of the Andaman Sea. *Indian Journal of Marine Sciences*, 10: 285–288.
- 490  
491 Bai L, Wang X, Zhou Y, Lin S, Meng F & Fontoura P (2020) *Moebjergarctus clarionclippertonensis*, a new abyssal  
492 tardigrade (Arthrotardigrada, Halechiniscidae, Euclavarctinae) from the Clarion-Clipperton Fracture Zone, North-  
493 East Pacific. *Zootaxa*, 4755(3): 561–575. DOI: <https://doi.org/10.11646/zootaxa.4755.3.8>
- 494  
495 Bluhm H (2001) Re-establishment of an abyssal megabenthic community after experimental physical disturbance of the  
496 seafloor. *Deep-Sea Research II*, 48: 3841–3868. DOI: [https://doi.org/10.1016/S0967-0645\(01\)00070-4](https://doi.org/10.1016/S0967-0645(01)00070-4)
- 497  
498 Bluhm H, Schriever G & Thiel H (1995) Megabenthic recolonization in an experimentally disturbed abyssal manganese  
499 nodule area. *Marine Georesources & Geotechnology*, 13: 393–416. DOI:  
500 <https://doi.org/10.1080/10641199509388295>
- 501  
502 Bonaglia S, Nascimento FJA, Bartoli M, Klawonn I & Brüchert V (2014) Meiofauna increases bacterial denitrification  
503 in marine sediments. *Nature Communications*, 5: 5133. DOI: <https://doi.org/10.1038/ncomms6133>
- 504

- 505 Bonifácio P, Martínez Arbizu P & Menot L (2020) Alpha and beta diversity patterns of polychaete assemblages across  
506 the nodule province of the eastern Clarion-Clipperton Fracture Zone (equatorial Pacific). *Biogeosciences*, 17: 865–  
507 886. DOI: <https://doi.org/10.5194/bg-17-865-2020>  
508
- 509 Bonifácio P & Menot L (2019) New genera and species from the equatorial Pacific provide phylogenetic insights into  
510 deep-sea Polynoidae (Annelida). *Zoological Journal of the Linnean Society*, 185: 555–635. DOI:  
511 <https://doi.org/10.1093/zoolinnean/zly063>  
512
- 513 Chim CK & Tong SJW (2020) Two new species of paratanaoid tanaidaceans of the family *incertae sedis* (Crustacea:  
514 Peracarida) from polymetallic nodule fields in the eastern Clarion-Clipperton Fracture Zone. *Zootaxa*, 4758: 461–  
515 485. DOI: <https://doi.org/10.11646/zootaxa.4758.3.3>  
516
- 517 Cho DH, Wi JH & Suh H (2016) Two new species of the deep-sea genus *Parameiropsis* (Copepoda: Harpacticoida)  
518 from the eastern central Pacific. *Zootaxa*, 4132: 521–539. DOI: <https://doi.org/10.11646/zootaxa.4132.4.4>  
519
- 520 Christodoulou M, O'Hara T, Hugall AF, Khodami S, Rodrigues CF, Hilario A, Vink A & Martínez Arbizu P (2020)  
521 Unexpected high abyssal ophiuroid diversity in polymetallic nodule fields of the northeast Pacific Ocean and  
522 implications for conservation. *Biogeosciences*, 17: 1845–1876. DOI: <https://doi.org/10.5194/bg-17-1845-2020>  
523
- 524 Chuar CH, Tong SJW, Chim CK, Wong HPS & Tan KS (2020) Abyssal macrofaunal community structure in the  
525 polymetallic nodule exploration area at the easternmost region of the Clarion-Clipperton Fracture Zone, Pacific  
526 Ocean. *Deep Sea Research Part I: Oceanographic Research Papers*, 161: 103284. DOI:  
527 <https://doi.org/10.1016/j.dsr.2020.103284>  
528
- 529 Clarke KR & Gorley RN (2015) PRIMER v7: user manual/tutorial. PRIMER-E Ltd, United Kingdom, 296 pp.  
530
- 531 Cordier T, Angeles IB, Henry N, Lejzerowicz F, Berney C, Morard R, Brandt A, Cambon-Bonavita M, Guidi L,  
532 Lombard F, Martínez Arbizu P, Massana R, Orejas C, Poulain J, Smith CR, Wincker P, Arnaud-Haond S, Gooday  
533 AJ, de Vargas C & Pawlowski J (2022) Patterns of eukaryotic diversity from the surface to the deep-ocean  
534 sediment. *Science Advances*, 8: eabj9309. DOI: <https://doi.org/10.1126/sciadv.abj9309>  
535
- 536 De Smet B, Pape E, Riehl T, Bonifácio P, Colson L & Vanreusel A (2017) The community structure of deep-sea  
537 macrofauna associated with polymetallic nodules in the eastern part of the Clarion-Clipperton Fracture Zone.  
538 *Frontiers in Marine Science*, 4: 103. DOI: <https://doi.org/10.3389/fmars.2017.00103>  
539
- 540 De Smet B, Simon-Lledó E, Mevenkamp L, Pape E, Pasotti F, Jones DOB & Vanreusel A (2021) The megafauna  
541 community from an abyssal area of interest for mining of polymetallic nodules. *Deep-Sea Research Part 1*, 172:  
542 103530. DOI: <https://doi.org/10.1016/j.dsr.2021.103530>  
543
- 544 Drennan R, Wiklund H, Rabone M, Georgieva MN, Dahlgren TG & Glover AG (2021) *Neanthes goodayi* sp. nov.  
545 (Annelida, Nereididae), a remarkable new annelid species living inside deep-sea polymetallic nodules. *European*  
546 *Journal of Taxonomy*, 760: 160–185. DOI: <https://doi.org/10.5852/ejt.2021.760.1447>  
547
- 548 Dugolinsky BK, Margolis SV & Dudley WC (1977) Biogenic influence on growth of manganese nodules. *Journal of*  
549 *Sedimentary Petrology*, 47: 428–445. DOI: <https://doi.org/10.1306/212F7194-2B24-11D7-8648000102C1865D>  
550
- 551 Fujimoto S & Murakami C (2020) A new genus and species of Nanaloricidae (Loricifera: Nanaloricida) from the  
552 Clarion-Clipperton Fracture Zone. *Zoologischer Anzeiger*, 289: 177–188. DOI:  
553 <https://doi.org/10.1016/j.jcz.2020.10.009>  
554
- 555 Fukushima T, Tsune A & Sugishima H (2022) Comprehensive understanding of seafloor disturbance and  
556 environmental impact scenarios. In: Sharma R (Ed) *Perspectives on deep-sea mining: sustainability, technology,*  
557 *environmental policy and management*. Springer, Cham, pp. 313–337. DOI: <https://doi.org/10.1007/978-3-030-87982-2>  
558
- 559
- 560 Gao AG, Wang CS, Yang JY, Wang ZP & He DH (2002) Distribution of deep-sea meiobenthos of the eastern and  
561 western portions of the COMRA's Pioneer Area. *Donghai Marine Science*, 20: 28–35.  
562
- 563 Gerlach SA (1971) On the importance of marine meiofauna for benthos communities. *Oecologia*, 6: 176–190. DOI:  
564 <https://doi.org/10.1007/BF00345719>  
565

- 566 Gheerardyn H & George KH (2019) Description of a new species of *Neoargestes* Drzycimski, 1967 (Copepoda,  
567 Harpacticoida, Argestidae) from the Clarion Clipperton Fracture Zone (Pacific Ocean), with remarks on the  
568 systematics of the genus. *Marine Biodiversity*, 49: 1891–1912. DOI: <https://doi.org/10.1007/s12526-019-00951-1>  
569
- 570 Giere O (2009) *Meiobenthology. The microscopic motile fauna of aquatic sediments* 2<sup>nd</sup> edition. Springer, Berlin, 527  
571 pp.  
572
- 573 Goineau A & Gooday AJ (2019) Diversity and spatial patterns of foraminiferal assemblages in the eastern Clarion–  
574 Clipperton zone. *Deep-Sea Research Part I*, 149: 103036. DOI: <https://doi.org/10.1016/j.dsr.2019.04.014>  
575
- 576 Gooday AJ, Durden JM, Holzmann M, Pawlowski J & Smith CR (2020) Xenophyophores (Rhizaria, Foraminifera),  
577 including four new species and two new genera, from the western Clarion-Clipperton Zone (abyssal equatorial  
578 Pacific). *European Journal of Protistology*, 75: 125715. DOI: <https://doi.org/10.1016/j.ejop.2020.125715>  
579
- 580 Gooday AJ & Goineau A (2019) The contribution of fine sieve fractions (63–150 µm) to foraminiferal abundance and  
581 diversity in an area of the eastern Pacific Ocean licensed for polymetallic nodule exploration. *Frontiers in Marine*  
582 *Science*, 6: 114. DOI: <https://doi.org/10.3389/fmars.2019.00114>  
583
- 584 Gooday AJ, Goineau A & Voltski I (2015) Abyssal foraminifera attached to polymetallic nodules from the eastern  
585 Clarion Clipperton Fracture Zone: a preliminary description and comparison with North Atlantic dropstone  
586 assemblages. *Marine Biodiversity*, 45: 391–412. DOI: <https://doi.org/10.1007/s12526-014-0301-9>  
587
- 588 Gooday AJ, Holzmann M, Caille C, Goineau A, Jones DOB, Kamenskaya O, Simon-Lledó E, Weber AAT &  
589 Pawlowski J (2017a) New species of the xenophyophore genus *Aschemonella* (Rhizaria: Foraminifera) from the  
590 areas of the abyssal eastern Pacific licensed for polymetallic nodule exploration. *Zoological Journal of the Linnean*  
591 *Society*, 182: 479–499. DOI: <https://doi.org/10.1093/zoolinnean/zlx052>  
592
- 593 Gooday AJ, Holzmann M, Caille C, Goineau A, Kamenskaya O, Weber AAT & Pawlowski J (2017b) Giant protists  
594 (xenophyophores, Foraminifera) are exceptionally diverse in parts of the abyssal eastern Pacific licensed for  
595 polymetallic nodule exploration. *Biological Conservation*, 207: 106–116. DOI:  
596 <https://doi.org/10.1016/j.biocon.2017.01.006>  
597
- 598 Gooday AJ, Holzmann M, Goineau A, Kamenskaya O, Melnik VF, Pearce RB, Weber AAT & Pawlowski J (2018a)  
599 Xenophyophores (Rhizaria, Foraminifera) from the eastern Clarion-Clipperton Zone (equatorial Pacific): the genus  
600 *Psammia*. *Protist*, 169: 926–957. DOI: <https://doi.org/10.1016/j.protis.2018.09.003>  
601
- 602 Gooday AJ, Holzmann M, Goineau A, Pearce RB, Voltski I, Weber AAT & Pawlowski J (2018b) Five new species and  
603 two new genera of xenophyophores (Foraminifera: Rhizaria) from part of the abyssal equatorial Pacific licensed for  
604 polymetallic nodule exploration. *Zoological Journal of the Linnean Society*, 183: 723–748. DOI:  
605 <https://doi.org/10.1093/zoolinnean/zlx093>  
606
- 607 Gooday AJ, Lejzerowicz F, Goineau A, Holzmann M, Kamenskaya O, Kitazato H, Lim SC, Pawlowski J, Radziejewska  
608 T, Stachowska Z & Wawrzyniak-Wydrowska B (2021) The biodiversity and distribution of abyssal benthic  
609 Foraminifera and their possible ecological roles: a synthesis across the Clarion-Clipperton Zone. *Frontiers in Marine*  
610 *Science*, 8: 634726. DOI: <https://doi.org/10.3389/fmars.2021.634726>  
611
- 612 Gooday AJ, Sykes D, Góral T, Zubkov MV & Glover AG (2018c) Micro-CT 3D imaging reveals the internal structure  
613 of three abyssal xenophyophore species (Protista, Foraminifera) from the eastern equatorial Pacific Ocean. *Scientific*  
614 *Reports*, 8: 12103. DOI: <https://doi.org/10.1038/s41598-018-30186-2>  
615
- 616 Grabowski RC (2014) Section 1.3.1: Measuring the shear strength of cohesive sediment in the field. In: Cook SJ, Clarke  
617 LE & Nield JM (Eds.) *Geomorphological Techniques* (Online Edition). British Society for Geomorphology,  
618 London.  
619
- 620 Guggolz T, Meißner K, Schwentner M, Dahlgren TG, Wiklund H, Bonifácio P & Brandt A (2020) High diversity and  
621 pan-oceanic distribution of deep-sea polychaetes: *Prionospio* and *Aurospio* (Annelida: Spionidae) in the Atlantic  
622 and Pacific Ocean. *Organisms Diversity & Evolution*, 20: 171–187. DOI: <https://doi.org/10.1007/s13127-020-00430-7>  
623
- 624  
625 Hannides AK & Smith CR (2003) The northeast abyssal Pacific plain. In: Black KD & Shimmield GB (Eds.)  
626 *Biogeochemistry of Marine Systems*. Blackwell Publishing Ltd, Oxford, pp. 208–237.  
627

- 628 Hauquier F, Macheriotou L, Bezerra TN, Egho G, Martínez Arbizu P & Vanreusel A (2019) Distribution of free-living  
629 marine nematodes in the Clarion-Clipperton Zone: implications for future deep-sea mining scenarios.  
630 Biogeosciences, 16: 3475–3489. DOI: <https://doi.org/10.5194/bg-16-3475-2019>  
631
- 632 Hecker B & Paul AZ (1979) Abyssal community structure of the benthic infauna of the eastern equatorial Pacific:  
633 DOMES sites A, B, and C. In: Bischoff JL & Piper DZ (Eds.) Marine Geology and Oceanography of the Pacific  
634 Manganese Nodule Province. Marine Science, vol. 9. Springer, Boston, MA, pp. 287–308.  
635
- 636 Hein JR, Mizell K, Koschinsky A & Conrad TA (2013) Deep-ocean mineral deposits as a source of critical metals for  
637 high- and green-technology applications: Comparison with land-based resources. Ore Geology Reviews, 51: 1–14.  
638 DOI: <https://doi.org/10.1016/j.oregeorev.2012.12.001>  
639
- 640 Ingels J, Vanreusel A, Pape E, Pasotti F, Martínez Arbizu P, Macheriotou L, Sørensen MV, Edgcomb VP, Sharma J,  
641 Sánchez N, Homoky WB, Leduc D, Gooday AJ, Pawlowski J, Dolan J, Schratzberger M, Gollner S, Schoenle A,  
642 Arndt H, Woulds C & Zeppilli D (2021) Ecological variables for deep-ocean monitoring must include microbiota  
643 and meiofauna for effective conservation. Nature Ecology & Evolution, 5: 27–19. DOI:  
644 <https://doi.org/10.1038/s41559-019-1091-z>  
645
- 646 ISA (2011) Environmental management plan for the Clarion Clipperton Zone, Kingston, Jamaica.  
647
- 648 ISA (2013) Recommendations for the guidance of contractors for the assessment of the possible environmental impacts  
649 arising from exploration for marine minerals in the Area International Seabed Authority, Kingston, Jamaica.  
650
- 651 ISA (2022) Exploration Contractors. URL: <https://isa.org.jm/exploration-contracts>. Accessed 1 July 2022.  
652
- 653 Janssen A, Stuckas H, Vink A & Martínez Arbizu P (2019) Biogeography and population structure of predominant  
654 macrofaunal taxa (Annelida and Isopoda) in abyssal polymetallic nodule fields: implications for conservation and  
655 management. Marine Biodiversity, 49: 2641–2658. DOI: <https://doi.org/10.1007/s12526-019-00997-1>  
656
- 657 Kaiser S, Kihara TC, Brix S, Mohrbeck I, Janssen A & Jennings RM (2021) Species boundaries and phylogeographic  
658 patterns in new species of *Nannoniscus* (Janiroidea: Nannoniscidae) from the equatorial Pacific nodule province  
659 inferred from mtDNA and morphology. Zoological Journal of the Linnean Society, 193: 1020–1071. DOI:  
660 <https://doi.org/10.1093/zoolinnean/zlaa174>  
661
- 662 Kaneko T, Maejima Y & Teishima H (1997) Abundance and vertical distribution of abyssal benthic fauna in the Japan  
663 Deep-Sea Impact Experiment. In: Proceedings of the Seventh International Offshore and Polar Engineering  
664 Conference. The International Society of Offshore and Polar Engineers, Honolulu, USA, pp. 475–480.  
665
- 666 Kersten O, Vetter EW, Jungbluth MJ, Smith CR & Goetze E (2019) Larval assemblages over the abyssal plain in the  
667 Pacific are highly diverse and spatially patchy. PeerJ: e7691. DOI: <http://doi.org/10.7717/peerj.7691>  
668
- 669 Kersten O, Smith CR & Vetter EW (2017) Abyssal near-bottom dispersal stages of benthic invertebrates in the Clarion-  
670 Clipperton polymetallic nodule province. Deep-Sea Research Part I, 127: 31–40. DOI:  
671 <https://doi.org/10.1016/j.dsr.2017.07.001>  
672
- 673 Kim DS, Hyun JH, Choi JW & Lee KY (2000) Meiobenthic fauna communities of the deep-sea sediments in the  
674 northeastern Pacific along a latitudinal transect. The Sea, 5: 245–254.  
675
- 676 Kim DS, Min WG, Lee KY & Kim KH (2004) Meiobenthic communities in the deep-sea sediment of the Clarion-  
677 Clipperton Fracture Zone in the northeast Pacific. Ocean and Polar Research, 26: 265–272. DOI:  
678 <https://doi.org/10.4217/OPR.2004.26.2.265>  
679
- 680 Kristensen RM, Gooday AJ & Goineau A (2019) Loricifera inhabiting spherical agglutinated structures in the abyssal  
681 eastern equatorial Pacific nodule fields. Marine Biodiversity, 49: 2455–2466. DOI: <https://doi.org/10.1007/s12526-019-00962-y>  
682
- 683 Laming SR, Christodoulou M, Martínez Arbizu P & Hilário A (2021) Comparative reproductive biology of deep-sea  
684 ophiuroids inhabiting polymetallic-nodule fields in the Clarion-Clipperton Fracture Zone. Frontiers in Marine  
685 Science, 8: 663798 DOI: <https://doi.org/10.3389/fmars.2021.663798>  
686
- 687 Langfelder LJ & Nivargikar VR (1967) Some factors influencing shear strength and compressibility of compacted soils.  
688 Highway Research Record, 177: 4–21.  
689



- 690  
691 Laroche O, Kersten O, Smith CR & Goetze E (2020) Environmental DNA surveys detect distinct metazoan  
692 communities across abyssal plains and seamounts in the western Clarion Clipperton Zone. *Molecular Ecology*, 29:  
693 4588–4604. DOI: <https://doi.org/10.1111/mec.15484>  
694
- 695 Leitner AB, Neuheimer AB, Donlon E, Smith CR & Drazen JC (2017) Environmental and bathymetric influences on  
696 abyssal bait-attending communities of the Clarion Clipperton Zone. *Deep-Sea Research Part I*, 125: 65–80. DOI:  
697 <https://doi.org/10.1016/j.dsr.2017.04.017>  
698
- 699 Lejzerowicz F, Gooday AJ, Barrenechea-Angeles I, Cordier T, Morard R, Apothéloz-Perret-Gentil L, Lins L, Menot L,  
700 Brandt A, Levin LA, Martínez Arbizu P, Smith CR & Pawlowski J (2021) Eukaryotic biodiversity and spatial  
701 patterns in the Clarion-Clipperton Zone and other abyssal regions: insights from sediment DNA and RNA  
702 metabarcoding. *Frontiers in Marine Science*, 8: 671033. DOI: <https://doi.org/10.3389/fmars.2021.671033>  
703
- 704 Lim SC, Wiklund H, Glover AG, Dahlgren TG & Tan KS (2017) A new genus and species of abyssal sponge  
705 commonly encrusting polymetallic nodules in the Clarion Clipperton Zone, east Pacific Ocean. *Systematics and*  
706 *Biodiversity*, 15: 507–519. DOI: <https://doi.org/10.1080/14772000.2017.1358218>  
707
- 708 Lindh MV, Maillot BM, Shulze CN, Gooday AJ, Amon DJ, Smith CR & Church MJ (2017) From the surface to the  
709 deep-sea: bacterial distributions across polymetallic nodule fields in the Clarion-Clipperton Zone of the Pacific  
710 Ocean. *Frontiers in Microbiology*, 8: 1696. DOI: <https://doi.org/10.3389/fmicb.2017.01696>  
711
- 712 Lindh MV, Maillot BM, Smith CR & Church MJ (2018) Habitat filtering of bacterioplankton communities above  
713 polymetallic nodule fields and sediments in the Clarion-Clipperton zone of the Pacific Ocean. *Environmental*  
714 *Microbiology Reports*, 10(2): 113–122. DOI: <https://doi.org/10.1111/1758-2229.12627>  
715
- 716 Lodge M, Johnson D, Le Gurun G, Wengler M, Weaver P & Gunn V (2014) Seabed mining: International Seabed  
717 Authority environmental management plan for the Clarion-Clipperton Zone. A partnership approach. *Marine Policy*,  
718 49: 66–72. DOI: <http://dx.doi.org/10.1016/j.marpol.2014.04.006>  
719
- 720 Löhr SC & Kennedy MJ (2015) Micro-trace fossils reveal pervasive reworking of Pliocene sapropels by low-oxygen-  
721 adapted benthic meiofauna. *Nature Communications*, 6: 6589. DOI: <https://doi.org/10.1038/ncomms7589>  
722
- 723 Mahatma R (2009) Meiofauna communities of the Pacific Nodule Province: abundance, diversity and community  
724 structure. PhD thesis, University of Oldenburg, Oldenburg, Germany  
725
- 726 Maljutina MV, Kihara TC & Brix S (2020) A new genus of Munnopsidae Lilljeborg, 1864 (Crustacea, Isopoda), with  
727 descriptions of two abyssal new species from the Clarion Clipperton Fracture Zone, north-eastern tropical Pacific.  
728 *Marine Biodiversity*, 50: 42. DOI: <https://doi.org/10.1007/s12526-020-01061-z>  
729
- 730 Martínez Arbizu, P & Haeckel M (2015) RV SONNE Fahrtbericht/Cruise Report SO239: EcoResponse assessing the  
731 ecology, connectivity and resilience of polymetallic nodule field systems, Balboa (Panama)–Manzanillo (Mexico)  
732 11.03.-30.04.2015. GEOMAR Report, N. Ser. 025. GEOMAR Helmholtz-Zentrum für Ozeanforschung, Kiel,  
733 Germany, 204 pp. DOI: [https://doi.org/10.3289/GEOMAR\\_REP\\_NS\\_25\\_2015](https://doi.org/10.3289/GEOMAR_REP_NS_25_2015)  
734
- 735 McIntyre AD & Warwick RM (1984) Meiofauna techniques. In: Holme NA & McIntyre AD (Eds.) *Methods for the*  
736 *study of marine benthos*. Blackwell Scientific Publishers, Oxford, pp. 217–244.  
737
- 738 Meadows PS, Reichelt AC, Meadows A & Waterworth JS (1994) Microbial and meiofaunal abundance, redox  
739 potential, pH and shear strength profiles in deep sea Pacific sediments. *Journal of the Geological Society, London*,  
740 151: 377–390. DOI: <https://doi.org/10.1144/gsjgs.151.2.0377>  
741
- 742 Mercado-Salas NF, Khodami S & Martínez Arbizu P (2019) Convergent evolution of mouthparts morphology between  
743 Siphonostomatoida and a new genus of deep-sea Aegisthidae Giesbrecht, 1893 (Copepoda: Harpacticoida). *Marine*  
744 *Biodiversity*, 49: 1635–1655. DOI: <https://doi.org/10.1007/s12526-018-0932-3>  
745
- 746 Miljutin DM, Miljutina MA, Martínez Arbizu P & Galéron J (2011) Deep-sea nematode assemblage has not recovered  
747 26 years after experimental mining of polymetallic nodules (Clarion-Clipperton Fracture Zone, tropical eastern  
748 Pacific). *Deep-Sea Research I*, 58: 885–897. DOI: <https://doi.org/10.1016/j.dsr.2011.06.003>  
749

- 750 Miljutin D, Miljutina M & Messié M (2015) Changes in abundance and community structure of nematodes from the  
 751 abyssal polymetallic nodule field, tropical northeast Pacific. *Deep-Sea Research I*, 106: 126–135. DOI:  
 752 <https://doi.org/10.1016/j.dsr.2015.10.009>  
 753
- 754 Min WG, Kim D, Rho HS, Chi SB & Son SK (2018) Distribution and variability of the meiobenthic assemblages near  
 755 the Korean polymetallic nodule claim area of the Clarion-Clipperton Fracture Zone (subequatorial NE Pacific).  
 756 *Ocean Science Journal*, 53: 315–336. DOI: <http://dx.doi.org/10.1007/s12601-018-0027-x>  
 757
- 758 Min WG, Kim DS & Kim WS (2004) Distribution of meiobenthic communities in the deep-sea floor of northeastern  
 759 Pacific seafloor along a latitudinal transect. *Ocean and Polar Research*, 26: 255–263. DOI:  
 760 <https://doi.org/10.4217/OPR.2004.26.2.255>  
 761
- 762 Mohrbeck I, Horton T, Jazdzewska AM & Martinez Arbizu P (2021) DNA barcoding and cryptic diversity of deep-sea  
 763 scavenging amphipods in the Clarion-Clipperton Zone (eastern equatorial Pacific). *Marine Biodiversity*, 51: 26.  
 764 DOI: <https://doi.org/10.1007/s12526-021-01170-3>  
 765
- 766 Mullineaux LS (1987) Organisms living on manganese nodules and crusts: distribution and abundance at three North  
 767 Pacific sites. *Deep-Sea Research*, 34: 165–184. DOI: [https://doi.org/10.1016/0198-0149\(87\)90080-X](https://doi.org/10.1016/0198-0149(87)90080-X)  
 768
- 769 Nascimento FJA, Näslund J & Elmgren R (2012) Meiofauna enhances organic matter mineralization in soft sediment  
 770 ecosystems. *Limnology and Oceanography*, 57: 338–346. DOI: <https://doi.org/10.4319/lo.2012.57.1.0338>  
 771
- 772 Nomaki H, Rastelli E, Alves A, Suga H, Ramos S, Kitahashi T, Tsuchiya M, Ogawa NO, Matsui Y, Seike K, Miyamoto  
 773 N, Corinaldesi C, Manea E, Ohkouchi N, Danovaro R, Nunoura T & Amaro T (2021) Abyssal fauna, benthic  
 774 microbes, and organic matter quality across a range of trophic conditions in the western Pacific Ocean. *Progress in*  
 775 *Oceanography*, 195: 102591. DOI: <https://doi.org/10.1016/j.pocean.2021.102591>  
 776
- 777 Pape E, Bezerra TN, Gheerardyn H, Buydens M, Kieswetter A & Vanreusel A (2021) Potential impacts of polymetallic  
 778 nodule removal on deep-sea meiofauna. *Scientific Reports*, 11: 19996. DOI: [https://doi.org/10.1038/s41598-021-](https://doi.org/10.1038/s41598-021-99441-3)  
 779 [99441-3](https://doi.org/10.1038/s41598-021-99441-3)  
 780
- 781 Pape E, Bezerra TN, Hauquier F & Vanreusel A (2017) Limited spatial and temporal variability in meiofauna and  
 782 nematode communities at distant but environmentally similar sites in an area of interest for deep-sea mining.  
 783 *Frontiers in Marine Science*, 4: 205. DOI: <https://doi.org/10.3389/fmars.2017.00205>  
 784
- 785 R Core Team (2019) R: A language and environment for statistical computing. R Foundation for Statistical Computing,  
 786 Vienna, Austria. URL: <https://www.R-project.org/>  
 787
- 788 Radziejewska T & Modlitba I (1999) Vertical distribution of meiobenthos in relation to geotechnical properties of deep  
 789 sea sediment in the IOM Pioneer Area (Clarion-Clipperton Fracture Zone, NE Pacific). In: *Proceedings of the Third*  
 790 *ISOPE Ocean Mining Symposium*. The International Society of Offshore and Polar Engineers, Goa, India, pp. 126–  
 791 130.  
 792
- 793 Radziejewska T, Rokicka-Praxmayer J & Stoyanova V (2001) IOM BIE Revisited: Meiobenthos at the IOM BIE site 5  
 794 years after the experimental disturbance. In: *Proceedings of the Fourth ISOPE Ocean Mining Symposium*. The  
 795 International Society of Offshore and Polar Engineers, Szczecin, Poland, pp. 63–68.  
 796
- 797 Radziejewska T (2002) Responses of deep-sea meiobenthic communities to sediment disturbance simulating effects of  
 798 polymetallic nodule mining. *International Review of Hydrobiology*, 87: 459–479. DOI:  
 799 [https://doi.org/10.1002/1522-2632\(200207\)87:4<457::AID-IROH457>3.0.CO;2-3](https://doi.org/10.1002/1522-2632(200207)87:4<457::AID-IROH457>3.0.CO;2-3)  
 800
- 801 Radziejewska T (2014) Meiobenthos in the sub-equatorial Pacific abyss. A proxy in anthropogenic impact evaluation.  
 802 Springer, Berlin, 105 pp.  
 803
- 804 Renaud-Mornant J & Goubault N (1990) Evaluation of abyssal meiobenthos in the eastern central Pacific (Clarion-  
 805 Clipperton fracture zone). *Progress in Oceanography*, 24: 317–329. DOI: [https://doi.org/10.1016/0079-](https://doi.org/10.1016/0079-6611(90)90041-Y)  
 806 [6611\(90\)90041-Y](https://doi.org/10.1016/0079-6611(90)90041-Y)  
 807
- 808 Richards AF & Parks JM (1976) Marine geotechnology: average sediment properties, selected literature and review of  
 809 consolidation, stability, and bioturbation-geotechnical interactions in the benthic layer. In: McCave IN (Ed.) *The*  
 810 *benthic boundary layer*. Plenum Press, New York and London, pp. 157–181.  
 811

- 812 Richardson MD, Briggs KB & Young DK (1985) Effects of biological activity by abyssal benthic macroinvertebrates  
813 on a sedimentary structure in the Venezuela Basin. *Marine Geology*, 68: 243–267. DOI:  
814 [https://doi.org/10.1016/0025-3227\(85\)90015-5](https://doi.org/10.1016/0025-3227(85)90015-5)  
815
- 816 Rolinski S, Segschneider J & Sündermann J (2001) Long-term propagation of tailings from deep sea mining under  
817 variable conditions by means of numerical simulations. *Deep-Sea Research II*, 48: 3469–3485. DOI:  
818 [https://doi.org/10.1016/S0967-0645\(01\)00053-4](https://doi.org/10.1016/S0967-0645(01)00053-4)  
819
- 820 Sánchez N, Pardos F & Martínez Arbizu P (2019) Deep-sea Kinorhyncha diversity of the polymetallic nodule fields at  
821 the Clarion-Clipperton Fracture Zone (CCZ). *Zoologischer Anzeiger*, 282: 88–105. DOI:  
822 <https://doi.org/10.1016/j.jcz.2019.05.007>  
823
- 824 Schratzberger M & Ingels J (2018) Meiofauna matters: the roles of meiofauna in benthic ecosystems. *Journal of*  
825 *Experimental Marine Biology and Ecology*, 502: 12–25. DOI: <https://doi.org/10.1016/j.jembe.2017.01.007>  
826
- 827 Shimada D, Takeda N, Tsune A & Murakami C (2020) Three species of free-living marine nematodes (Nematoda:  
828 Enoplida) from the Clarion-Clipperton Fracture Zone (CCFZ), North Pacific. *Zootaxa*, 4859: 507–526. DOI:  
829 <https://doi.org/10.11646/zootaxa.4859.4.3>  
830
- 831 Shirayama Y (1984) Vertical distribution of meiobenthos in the sediment profile in bathyal, abyssal and hadal deep sea  
832 systems of the western Pacific. *Oceanologica Acta*, 7: 113–121.  
833
- 834 Shirayama Y & Kojima S (1994) Abundance of deep-sea meiobenthos off Sanriku, northeastern Japan. *Journal of*  
835 *Oceanography*, 50: 109–117. DOI: <https://doi.org/10.1007/BF02233860>  
836
- 837 Simon-Lledó E, Pomee C, Ahokava A, Drazen JC, Leitner AB, Flynn A, Parianos J & Jones DOB (2020) Multi-scale  
838 variations in invertebrate and fish megafauna in the mid-eastern Clarion Clipperton Zone. *Progress in*  
839 *Oceanography*, 187: 102405. DOI: <https://doi.org/10.1016/j.pocean.2020.102405>  
840
- 841 Sinniger F, Pawlowski J, Harii S, Gooday AJ, Yamamoto H, Chevaldonné P, Cedhagen T, Carvalho G & Creer S  
842 (2016) Worldwide analysis of sedimentary DNA reveals major gaps in taxonomic knowledge of deep-sea benthos.  
843 *Frontiers in Marine Science*, 3: 92. DOI: <https://doi.org/10.3389/fmars.2016.00092>  
844
- 845 Smith CR, Berelson W, Demaster DJ, Dobbs FC, Hammond D, Hoover DJ, Pope RH & Stephens M (1997) Latitudinal  
846 variations in benthic processes in the abyssal equatorial Pacific: control by biogenic particle flux. *Deep-Sea*  
847 *Research II*, 44: 2295–2317. DOI: [https://doi.org/10.1016/S0967-0645\(97\)00022-2](https://doi.org/10.1016/S0967-0645(97)00022-2)  
848
- 849 Smith CR & Demopoulos AWJ (2003) The deep Pacific Ocean floor. In: Tyler PA (Ed.) *Ecosystems of the world*,  
850 Volume 28: *Ecosystems of the deep oceans*. Elsevier, Amsterdam, pp. 179–218.  
851
- 852 Smith CR, De Leo FC, Bernardino AF, Sweetman AK & Martínez Arbizu P (2008) Abyssal food limitation, ecosystem  
853 structure and climate change. *Trends in Ecology & Evolution*, 23: 518–528. DOI:  
854 <https://doi.org/10.1016/j.tree.2008.05.002>  
855
- 856 Snider LJ, Burnett BR & Hessler RR (1984) The composition and distribution of meiofauna and nanobiota in a central  
857 north Pacific deep-sea area. *Deep Sea Research Part A. Oceanographic Research Papers*, 31: 1225–1249. DOI:  
858 [https://doi.org/10.1016/0198-0149\(84\)90059-1](https://doi.org/10.1016/0198-0149(84)90059-1)  
859
- 860 Stratmann T, Lins L, Purser A, Marcon Y, Rodrigues CF, Ravara A, Cunha MR, Simon-Lledó E, Jones DOB,  
861 Sweetman AK, Köser K & van Oevelen D (2018) Abyssal plain faunal carbon flows remain depressed 26 years after  
862 a simulated deep-sea mining disturbance. *Biogeosciences*, 15: 4131–4145. DOI: <https://doi.org/10.5194/bg-15-4131-2018>  
863  
864
- 865 Stratmann T, Soetaert K, Kersken D & van Oevelen D (2021) Polymetallic nodules are essential for food-web integrity  
866 of a prospective deep-seabed mining area in Pacific abyssal plains. *Scientific Reports*, 11: 12238. DOI:  
867 <https://doi.org/10.1038/s41598-021-91703-4>  
868
- 869 Sweetman AK, Smith CR, Shulse CN, Maillot B, Lindh M, Church MJ, Meyer KS, van Oevelen D, Stratmann T &  
870 Gooday AJ (2019) Key role of bacteria in the short-term cycling of carbon at the abyssal seafloor in a low  
871 particulate organic carbon flux region of the eastern Pacific Ocean. *Limnology and Oceanography*, 64: 694–713.  
872 DOI: <https://doi.org/10.1002/lno.11069>  
873

- 874 Taboada S, Riesgo A, Wiklund H, Paterson GLJ, Koutsouveli V, Santodomingo N, Dale AC, Smith CR, Jones DOB,  
875 Dahlgren TG & Glover AG (2018) Implications of population connectivity studies for the design of marine  
876 protected areas in the deep sea: an example of a demosponge from the Clarion-Clipperton Zone. *Molecular Ecology*,  
877 27: 4657–4679. DOI: <https://doi.org/10.1111/mec.14888>  
878
- 879 Thiel H, Schriever G, Ahnert A, Bluhm H, Borowski C & Vopel K (2001) The large-scale environmental impact  
880 experiment DISCOL—reflection and foresight. *Deep Sea Research II*, 48: 3869–3882. DOI:  
881 [https://doi.org/10.1016/S0967-0645\(01\)00071-6](https://doi.org/10.1016/S0967-0645(01)00071-6)  
882
- 883 Thiel H, Schriever G, Bussau C & Borowski C (1993) Manganese nodule crevice fauna. *Deep-Sea Research I*, 40: 419–  
884 423. DOI: [https://doi.org/10.1016/0967-0637\(93\)90012-R](https://doi.org/10.1016/0967-0637(93)90012-R)  
885
- 886 Trask PD & Rolston JW (1950) Relation of strength and sediments to water content and grain size. *Science*, 111: 666–  
887 667.  
888
- 889 Trueblood DD & Ozturgut E (1997) The Benthic Impact Experiment: a study of the ecological impacts of deep seabed  
890 mining on abyssal benthic communities. In: *Proceedings of the Seventh International Offshore and Polar*  
891 *Engineering Conference*. The International Society of Offshore and Polar Engineers, Honolulu, USA, pp. 481–487.  
892
- 893 Trueblood DD, Ozturgut E, Pilipchuk M & Gloumov IF (1997) The ecological impacts of the joint U.S.-Russian  
894 Benthic Impact Experiment. In: *Proceedings of the Second Ocean Mining Symposium*. The International Society of  
895 Offshore and Polar Engineers, Seoul, Korea, pp. 139–145.  
896
- 897 Uhlenkott K, Vink A, Kuhn T, Gillard B & Martínez Arbizu P (2020) Meiofauna in a potential deep-sea mining area—  
898 influence of temporal and spatial variability on small-scale abundance models. *Diversity*, 13: 3. DOI:  
899 <https://doi.org/10.3390/d13010003>  
900
- 901 Vanreusel A, Hilario A, Ribeiro PA, Menot L & Martínez Arbizu P (2016) Threatened by mining, polymetallic nodules  
902 are required to preserve abyssal epifauna. *Scientific Reports*, 6: 26808. DOI: <https://doi.org/10.1038/srep26808>  
903
- 904 Vanreusel A, Fonseca G, Danovaro R, da Silva MC, Esteves AM, Ferrero T, Gad G, Galtsova V, Gambi C, da Fonsêca  
905 Genevois V, Ingels J, Ingole B, Lampadariou N, Merckx B, Miljutin D, Miljutina M, Muthumbi A, Netto S,  
906 Portnova D, Radziejewska T, Raes M, Tchesunov A, Vanaverbeke J, Gaever SV, Venekey V, Bezerra TN, Flint H,  
907 Copley J, Pape E, Zeppilli D, Martinez PA & Galeron J (2010) The contribution of deep-sea macrohabitat  
908 heterogeneity to global nematode diversity. *Marine Ecology*, 31: 6–20. DOI: <https://doi.org/10.1111/j.1439-0485.2009.00352.x>  
909
- 910  
911 Veillette J, Juniper SK, Gooday AJ & Sarrazin J (2007a) Influence of surface texture and microhabitat heterogeneity in  
912 structuring nodule faunal communities. *Deep Sea Research Part I: Oceanographic Research Papers*, 54: 1963–1943.  
913 DOI <https://doi.org/10.1016/j.dsr.2007.06.012>  
914
- 915 Veillette J, Sarrazin J, Gooday AJ, Galéron J, Caprais J, Vangriesheim A, Étoubleau J, Christian JR & Juniper SK  
916 (2007b). Ferromanganese nodule fauna in the tropical north Pacific Ocean: species richness, faunal cover and spatial  
917 distribution. *Deep Sea Research Part I: Oceanographic Research Papers*, 54: 1912–1935. DOI:  
918 <https://doi.org/10.1016/j.dsr.2007.06.011>  
919
- 920 Wang XG, Zhou YD, Zhang DS, Hong LS & Wang CS (2013) A study of meiofauna in the COMRA's contracted area  
921 during the summer of 2005. *Acta Ecologica Sinica*, 33: 492–500. DOI: <https://doi.org/10.5846/stxb201111251801>  
922
- 923 Washburn TW, Menot L, Bonifácio P, Pape E, Blazewicz M, Bribiesca-Contreras G, Dahlgren TG, Fukushima T,  
924 Glover AG, Ju SJ, Kaiser S, Yu OH & Smith CR (2021) Patterns of macrofaunal biodiversity across the Clarion-  
925 Clipperton Zone: an area targeted for seabed mining. *Frontiers in Marine Science*, 8: 626571. DOI:  
926 <https://doi.org/10.3389/fmars.2021.626571>  
927
- 928 Wear EK, Church MJ, Orcutt BN, Shulse CN, Lindh MV & Smith CR (2021) Bacterial and archaeal communities in  
929 polymetallic nodules, sediments, and bottom waters of the abyssal Clarion-Clipperton Zone: emerging patterns and  
930 future monitoring considerations. *Frontiers in Marine Science*, 8: 634803. DOI:  
931 <https://doi.org/10.3389/fmars.2021.634803>  
932
- 933 Wiklund H, Neal L, Glover AG, Drennan R, Rabone M & Dahlgren TG (2019) Abyssal fauna of polymetallic nodule  
934 exploration areas, eastern Clarion-Clipperton Zone, central Pacific Ocean: Annelida: Capitellidae, Opheliidae,  
935 Scalibregmatidae, and Traviisiidae. *Zookeys*, 883: 1–82. DOI: <https://doi.org/10.3897/zookeys.883.36193>

- 936  
937 Wilson GDF (1990) Biological evaluation of a Preservational Reserve Area (“BEPRA 1”). Cruise Report and Interim  
938 report on laboratory analysis, Scripps Institution of Oceanography, La Jolla, California, USA, 34 pp.  
939
- 940 Wilson GDF (1992) Biological evaluation of a Preservational Reserve Area: faunal data and comparative analysis.  
941 Australian Museum, Sydney.  
942
- 943 Wilson GDF (2017) Macrofauna abundance, species diversity and turnover at three sites in the Clipperton-Clarion  
944 Fracture Zone. *Marine Biodiversity*, 47: 323–347. DOI: <https://doi.org/10.1007/s12526-016-0609-8>  
945
- 946 Wilson GDF & Hessler RR (1987) The effects of manganese nodule test mining on the benthic fauna in the north  
947 equatorial Pacific. In: Spiess FN, Hessler R, Wilson G & Weydert M (Eds.) *Environmental Effects of Deep Sea*  
948 *Dredging. Final Report to the National Oceanic and Atmospheric Administration on Contract Number 83-SAC-*  
949 *00659. Scripps Institute of Oceanography, La Jolla, CA, pp. 24–86.*  
950
- 951 Woods DR & Tietjen JH (1985) Horizontal and vertical distribution of meiofauna in the Venezuela Basin. *Marine*  
952 *Geology*, 68: 233–241. DOI: [https://doi.org/10.1016/0025-3227\(85\)90014-3](https://doi.org/10.1016/0025-3227(85)90014-3)  
953
- 954 Zeng Q, Huang D, Lin R & Wang J (2018) Deep-sea metazoan meiofauna from a polymetallic nodule area in the  
955 Central Indian Ocean Basin. *Marine Biodiversity*, 48: 395–405. DOI: <https://doi.org/10.1007/s12526-017-0778-0>  
956
- 957 Zhao M, Liu Q, Zhang D, Liu Z, Wang C & Liu X (2020) Deep-sea meiofauna assemblages with special reference to  
958 marine nematodes in the Caiwei Guyot and a Polymetallic Nodule Field in the Pacific Ocean. *Marine Pollution*  
959 *Bulletin*, 160: 111564. DOI: <https://doi.org/10.1016/j.marpolbul.2020.111564>  
960  
961  
962  
963  
964  
965  
966  
967  
968  
969  
970  
971  
972  
973  
974  
975  
976  
977  
978  
979  
980  
981  
982  
983  
984  
985  
986  
987  
988  
989  
990  
991  
992  
993  
994  
995  
996  
997

998 **Appendix: Supplementary data**999  
1000  
1001  
1002**Table S1.**

Spearman rank correlations and corresponding p-values between environmental variables.

	<b>Nodule cover</b>		<b>Nodule weight</b>		<b>Nodule volume</b>	
	rho	p-value	rho	p-value	rho	p-value
<b>Shear strength</b>	0.29	0.35	0.04	0.90	0.07	0.83
<b>Nodule cover</b>	-	-	0.36	0.25	0.40	0.20
<b>Nodule weight</b>	-	-	-	-	0.99	< 0.01

1003  
1004  
1005

Journal Pre-proof

1006  
1007  
1008**Table S2.**  
Raw data.

Station	<b>1</b>		<b>1</b>		<b>1</b>		<b>1</b>		<b>2</b>		<b>2</b>		<b>2</b>		<b>2</b>		<b>3</b>		<b>3</b>		<b>3</b>		<b>3</b>	
	C03-SGN 051-B 0-2cm	C03-SGN 051-C 2-5cm	C05-SGN 052-B 0-2cm	C05-SGN 052-C 2-5cm	C07-SGN 053-B 0-2cm	C07-SGN 053-C 2-5cm	C12-SGN 054-B 0-2cm	C12-SGN 054-C 2-5cm	C02-SGN 077-B 0-2cm	C02-SGN 077-C 2-5cm	C07-SGN 078-B 0-2cm	C07-SGN 078-C 2-5cm	C11-SGN 079-B 0-2cm	C11-SGN 079-C 2-5cm	C12-SGN 080-B 0-2cm	C12-SGN 080-C 2-5cm	C01-SGN 058-A 0-2cm	C01-SGN 058-B 2-5cm	C03-SGN 059-A 0-2cm	C03-SGN 059-B 2-5cm	C06-SGN 060-B 0-2cm	C06-SGN 060-C 2-7cm	C07-SGN 061-B 0-2cm	C07-SGN 061-C 2-5cm
<b>Nematoda</b>	1663	152	1149	154	1071	268	1668	387	1369	543	843	280	763	463	831	561	1102	774	1031	446	1059	812	1541	386
<b>Nauplii</b>	88	6	108	2	102	10	121	17	164	8	71	7	86	22	59	18	28	6	23	14	96	49	88	10
<b>Unknown</b>	3	1	9	3	26		72				4	4	1	13	3	2					2		2	3
<b>Copepoda</b>	119	3	70	6	60	15	84	13	108	12	77	4	75	18	54	13	40	23	26	9	60	25	83	7
<b>Gastrotricha</b>			1	1	4		2	1	1	2		2	1	2			2				1		2	
<b>Loricifera</b>	1		2						2		4		19	2	10				1	2		11	3	1
<b>Rotifera</b>								1			1													
<b>Tantulocarida</b>	5		4	1			1	1	4		1		3	1	1						2	1	1	
<b>Tardigrada</b>	3		1						6		6		1		3	6					1	5	3	
<b>Acari</b>	2				1	1	1	1			1	2	7		1	1	1		5		2		4	
<b>Amphipoda</b>																								
<b>Annelida</b>	30	1	12	3	18	2	16	0	10	2	17	0	9	3	12	4	1	5	6		12	5	8	1
<b>Bivalvia</b>	1		1								1				2				1					
<b>Cumacea</b>																								
<b>Isopoda</b>											1	1	1	1	1	2			1		1	1	1	
<b>Kinorhyncha</b>	3		4				1				2				2		2	1	2	1	3		3	
<b>Ostracoda</b>	7		3	1	5	2	16		6		5		4		2	1	7	3	1		4	3	7	
<b>Tanaidacea</b>	1		3				3		2	1	1				1		1				2		3	1
<b>Platyhelminthes</b>																								
<b>Asteroidae</b>																								
<b>Nemertea</b>															11						1		2	
<b>Gastropoda</b>																								
<b>Sipuncula</b>																								

1009  
1010  
1011

Table S2. (continued)

Raw data.

Station	4		4		4		4		5		5		5		5		6		6		6		6	
	C01-SGN 071- B 0- 2cm	C01-SGN 071- C 2- 5cm	C03-SGN 072- B 0- 2cm	C03-SGN 072- C 2- 5cm	C07-SGN 073- B 0- 2cm	C07-SGN 073- C 2- 5cm	C12-SGN 074- B 0- 2cm	C12-SGN 074- C 2- 5cm	C04-SGN 086- B 0- 2cm	C04-SGN 086- C 2- 5cm	C05-SGN 087- B 0- 2cm	C05-SGN 087- C 2- 5cm	C06-SGN 088- B 0- 2cm	C06-SGN 088- C 2- 5cm	C12-SGN 089- B 0- 2cm	C12-SGN 089- C 2- 5cm	C04-SGN 093- B 0- 2cm	C04-SGN 093- C 2- 5cm	C08-SGN 094- B 0- 2cm	C08-SGN 094- C 2- 5cm	C09-SGN 095- B 0- 2cm	C09-SGN 095- C 2- 5cm	C12-SGN 096- B 0- 2cm	C12-SGN 096- C 2- 5cm
<b>Nematoda</b>	1177	464	1506	320	1319	168	968	345	1393	445	1449	241	1236	295	1062	129	1084	431	1459	361	1158	289	1051	555
<b>Nauplii</b>	43	6	88	11	94	8	97	7	73	7	126	10	61	3	76	1	53	7	49	8	20	3	32	11
<b>Unknown</b>			7	1	23		4	1			2	1		1	2		7		4		2		1	1
<b>Copepoda</b>	37	11	71	14	46	5	47	10	51	14	68	17	75	4	86	5	37	13	45	10	50	7	46	18
<b>Gastrotricha</b>	1				1		1				3		2		1									
<b>Loricifera</b>	2		2	1	5		4		2		4	1								2	1		1	
<b>Rotifera</b>																								
<b>Tantulocarida</b>		1	2		2		3		2		2		1		2		3		3					
<b>Tardigrada</b>	5					1	2		8		10		4		14	1				3				
<b>Acari</b>		1			5		2						2						1	1	1			
<b>Amphipoda</b>																								
<b>Annelida</b>	9	2	19		14	0	15	3	13	0	38	3	15	1	28		8	1	11	1	6	0	12	3
<b>Bivalvia</b>			1								1								1					
<b>Cumacea</b>															1									
<b>Isopoda</b>	2		1		1		1						2		2									
<b>Kinorhyncha</b>			2		2		1		1		3		2		3				1					
<b>Ostracoda</b>	1		6	2	3		3		7		4		1		2		5		3		2		1	
<b>Tanaidacea</b>			3	1	1	1	1										1		1		1		1	
<b>Platyhelminthes</b>																								
<b>Asteroidae</b>																								
<b>Nemertea</b>					4																			
<b>Gastropoda</b>	1		2																					
<b>Sipuncularia</b>													2											



1012  
1013  
1014

Table S2. (continued)

Raw data.

Station	7							8							9									
	C02-SGN	C02-SGN	C05-SGN	C05-SGN	C09-SGN	C09-SGN	C11-SGN	C11-SGN	C01-SGN	C01-SGN	C02-SGN	C02-SGN	C04-SGN	C04-SGN	C05-SGN	C05-SGN	C03-SGN	C03-SGN	C04-SGN	C04-SGN	C08-SGN	C08-SGN	C09-SGN	C09-SGN
Sample	153-B	153-C	154-B	154-C	155-B	155-C	156-B	156-C	169-A	169-B	170-A	170-B	171-A	171-B	172-A	172-B	143-B	143-C	144-B	144-C	145-B	145-C	146-B	146-C
Fraction	0-2cm	2-5cm	0-2cm	2-5cm	0-2cm	2-5cm	0-2cm	2-5cm	0-2cm	2-5cm	0-2cm	2-5cm	0-2cm	2-5cm	0-2cm	2-5cm	0-2cm	2-5cm	0-2cm	2-5cm	0-2cm	2-5cm	0-2cm	2-5cm
<b>Nematoda</b>	1545	809	682	241	1862	196	914	305	1316	857	1193	734	761	779	1764	844	1397	666	1341	184	1412	272	1274	176
<b>Nauplii</b>	48	21	77	17	175	14	98	4	62	13	111	14	70	15	135	21	53	8	130	15	97	8	111	9
<b>Unknown</b>	1		6	6	5	1	10				1	2	5	4	2				16	3	18	1	9	5
<b>Copepoda</b>	62	14	73	23	135	20	109	12	135	17	102	24	80	22	117	16	85	17	80	15	66	10	93	7
<b>Gastrotricha</b>	2				2		4				1		4	2	2		1	1	1		3		2	
<b>Loricifera</b>			3	1	3		1	2		1		9	1	2	4	2	1		32	15	13	17	18	7
<b>Rotifera</b>																								
<b>Tantulocarida</b>	2	1	1		1	1					3				4		1		3		4	1	4	
<b>Tardigrada</b>					1		1	1	3		2		7	1	9	14	2		5		1		1	
<b>Acari</b>							1	1			3		1											
<b>Amphipoda</b>																								
<b>Annelida</b>	7	2	7	2	33	0	38	3	20	4	12	2	10	6	19	5	22	5	25	0	20		27	3
<b>Bivalvia</b>							1				1		3		2			1					1	
<b>Cumacea</b>																								
<b>Isopoda</b>		1	1	1	4		1				1				1	1			1	1			3	
<b>Kinorhyncha</b>	2		3		1				2	1	2	1	2		4									
<b>Ostracoda</b>	3		5	2	8	1	14		4	3	5	1	3	1	10		3	2	2	11	4		4	
<b>Tanaidacea</b>		1					5		1		1		1	1	1		1		5		2		1	
<b>Platyhelminthes</b>											1													
<b>Asteroidae</b>																								
<b>Nemertea</b>																					3			
<b>Gastropoda</b>					2																			
<b>Sipuncularia</b>					1																			

1015  
1016  
1017

Table S2. (continued)

Raw data.

Station	10 C03- SGN	10 C03- SGN	10 C10- SGN	10 C10- SGN	10 C11- SGN	10 C11- SGN	10 C12- SGN	10 C12- SGN	11 C01- SGN	11 C01- SGN	11 C02- SGN	11 C02- SGN	11 C06- SGN	11 C06- SGN	11 C07- SGN	11 C07- SGN	12 C05- SGN	12 C05- SGN	12 C07- SGN	12 C07- SGN	12 C10- SGN	12 C10- SGN	12 C11- SGN	12 C11- SGN
Sample	159- B	159- C	160- B	160- C	161- B	161- C	162- B	162- C	178- B	178- C	179- B	179- C	180- B	180- C	181- B	181- C	184- B	184- C	185- B	185- C	186- B	186- C	187- B	187- C
Fraction	0- 2cm	2- 5cm	0- 2cm	2- 5cm	0- 2cm	2- 5cm	0- 2cm	2- 5cm	0- 2cm	2- 5cm	0- 2cm	2- 5cm	0- 2cm	2- 5cm	0- 2cm	2- 5cm	0- 2cm	2- 5cm	0- 2cm	2- 5cm	0- 2cm	2- 5cm	0- 2cm	2- 5cm
<b>Nematoda</b>	1603	287	1639	200	1145	333	1157	319	1532	85	1028	248	975	539	1320	124	736	585	1124	347	1148	735	899	255
<b>Nauplii</b>	62	10	225	7	112	8	65	15	30	2	60	13	84	22	89	1	14	9	38	7	42	25	36	6
<b>Unknown</b>	1		9	4	9	5	4	3			9		1	19		3			26	6	4	1	2	
<b>Copepoda</b>	70	9	138	6	64	6	39	9	47	2	33	9	54	17	46	3	28	12	35	16	28	20	32	6
<b>Gastrotricha</b>			2		1		1						3					1	3			2		
<b>Loricifera</b>	1		6	1	5		10	1	3		4		8	4	11				1				1	
<b>Rotifera</b>			1																					
<b>Tantulocarida</b>	3		8	1	6		3				1	1	6		3	1						1	1	
<b>Tardigrada</b>	3		2		4		15		2				2		4		3	1	9		2	3	1	
<b>Acari</b>					1										5		1					1		
<b>Amphipoda</b>	1																							
<b>Annelida</b>	18	1	47	2	6		8	2	41	0	11	5	28	11	11		8	2	26	5	11	7	9	1
<b>Bivalvia</b>			2		3			1							2		1							
<b>Cumacea</b>																								
<b>Isopoda</b>							1							1			1					1		
<b>Kinorhyncha</b>			3										1		1				3					
<b>Ostracoda</b>	4		8		4		6		4		3	1	6		7				1	1		1	2	
<b>Tanaidacea</b>	4		3		3		2		1		1				1				1	1	3	1	2	1
<b>Platyhelminthes</b>																								
<b>Asteroida</b>			1																					
<b>Nemertea</b>																								
<b>Gastropoda</b>									1				1											
<b>Sipuncula</b>																								

1018  
1019  
1020**Table S3.**  
Mean percentage of meiobenthos across the 12 stations from the 0–5 cm sediment layer.

	Station												mean	s.d.
	1	2	3	4	5	6	7	8	9	10	11	12		
<b>Nematoda</b>	85.36	84.61	91.01	88.93	87.56	92.78	84.24	87.43	85.21	86.37	88.81	91.96	87.86	2.90
<b>Nauplii</b>	6.11	6.39	3.83	5.11	5.00	2.63	6.31	4.68	5.65	6.33	4.60	2.75	4.95	1.33
<b>Unknown</b>	1.40	0.46	0.08	0.52	0.09	0.22	0.50	0.18	0.69	0.46	0.48	0.59	0.47	0.35
<b>Copepoda</b>	4.89	5.46	3.37	3.40	4.64	3.31	6.39	5.52	4.78	4.25	3.18	2.83	4.34	1.13
<b>Gastrotricha</b>	0.13	0.13	0.06	0.05	0.08	0.00	0.11	0.11	0.10	0.05	0.04	0.09	0.08	0.04
<b>Loricifera</b>	0.04	0.60	0.22	0.20	0.09	0.06	0.17	0.20	1.37	0.33	0.45	0.04	0.31	0.38
<b>Rotifera</b>	0.01	0.02	0.00	0.00	0.00	0.00	0.00	0.00	0.00	0.01	0.00	0.00	0.00	0.01
<b>Tantulocarida</b>	0.16	0.15	0.05	0.12	0.10	0.08	0.07	0.07	0.17	0.27	0.18	0.03	0.12	0.07
<b>Tardigrada</b>	0.06	0.34	0.10	0.12	0.55	0.04	0.04	0.36	0.12	0.34	0.12	0.29	0.21	0.16
<b>Acari</b>	0.08	0.20	0.16	0.12	0.03	0.04	0.03	0.05	0.00	0.01	0.08	0.03	0.07	0.06
<b>Amphipoda</b>	0.00	0.00	0.00	0.00	0.00	0.00	0.00	0.00	0.00	0.01	0.00	0.00	0.00	0.00
<b>Annelida</b>	1.10	0.90	0.47	0.89	1.41	0.60	1.29	0.83	1.31	1.00	1.58	1.07	1.04	0.33
<b>Bivalvia</b>	0.03	0.04	0.02	0.01	0.01	0.01	0.02	0.07	0.03	0.08	0.03	0.02	0.03	0.02
<b>Cumacea</b>	0.00	0.00	0.00	0.00	0.02	0.00	0.00	0.00	0.00	0.00	0.00	0.00	0.00	0.01
<b>Isopoda</b>	0.00	0.11	0.05	0.07	0.06	0.00	0.11	0.03	0.07	0.02	0.01	0.03	0.05	0.04
<b>Kinorhyncha</b>	0.11	0.07	0.15	0.07	0.13	0.01	0.10	0.13	0.00	0.03	0.03	0.05	0.07	0.05
<b>Ostracoda</b>	0.43	0.27	0.30	0.20	0.19	0.16	0.50	0.28	0.34	0.28	0.32	0.08	0.28	0.11
<b>Tanaidacea</b>	0.09	0.07	0.08	0.09	0.00	0.06	0.09	0.06	0.12	0.15	0.05	0.15	0.08	0.04
<b>Platyhelminthes</b>	0.00	0.00	0.00	0.00	0.00	0.00	0.00	0.01	0.00	0.00	0.00	0.00	0.00	0.00
<b>Asteroidea</b>	0.00	0.00	0.00	0.00	0.00	0.00	0.00	0.00	0.00	0.01	0.00	0.00	0.00	0.00
<b>Nemertea</b>	0.00	0.17	0.03	0.06	0.00	0.00	0.00	0.00	0.04	0.00	0.00	0.00	0.03	0.05
<b>Gastropoda</b>	0.00	0.00	0.00	0.04	0.00	0.00	0.02	0.00	0.00	0.00	0.03	0.00	0.01	0.01
<b>Sipuncula</b>	0.00	0.00	0.00	0.00	0.03	0.00	0.01	0.00	0.00	0.00	0.00	0.00	0.00	0.01

1021

1022  
1023  
1024**Table S4.**Average within-group similarity based on relative abundances (4<sup>th</sup>-root transformed) and absolute abundances (log x+1 transformed).

	Relative abundance	Absolute abundance
S01	83.46	84.70
S02	84.81	83.23
S03	81.02	80.75
S04	83.94	83.10
S05	84.54	85.15
S06	87.01	87.54
S07	80.55	81.48
S08	85.23	84.52
S09	88.05	86.10
S10	84.85	84.18
S11	81.38	82.46
S12	80.69	81.97

1025  
1026  
1027  
1028  
1029  
1030  
1031  
1032  
1033**Table S5.**

Calculations for bar chart. PRZ1302, WS1303, JET, KODOS, NIXO, ECHO, BGR\_RA and OMS were taken or calculated from their reference papers. The means for COMRA West, COMRA East, IFREMER, GSR (B4), GSR (B6) and BGR\_PA were calculated from the means obtained from their relevant studies. The IOM-BIE value was calculated using data from Hauquier et al. (2019), Radziejewska (2014), and the means obtained from C1, C2 and C3 in (Radziejewska et al., 2001; Radziejewska, 2002, 2014). The value for NOAA-BIE was obtained by averaging the means of the min and max values reported in Radziejewska (2014). Abundance presented as the number of individuals (ind.) per 10 cm<sup>2</sup>. s.d. = standard deviation.

	References	Data in references		Remarks	Used in Figure 6	
		Abundance $\pm$ s.d.	n		Abundance $\pm$ s.d.	n
<b>PRZ1302</b>	Zhao et al., 2020	4.97	1		4.97	1
<b>WS1303</b>	Zhao et al., 2020	45.3	1		45.3	1
<b>JET1</b>	Kaneko et al., 1997	101.0 $\pm$ 55.9	44 subcores		101.0 $\pm$ 55.9	44
<b>KODOS</b>	Kim et al., 2000; Kim et al., 2004; Min et al., 2004; Min et al., 2018	84.25 $\pm$ 52.72	29	modified original data to exclude the Foraminifera	84.25 $\pm$ 52.72	29
<b>NIXO</b>	Renaud-Mornant & Gourbault, 1990	160 $\pm$ 45.15	17	modified original data by adding subsamples A,B from the same box corer together used only the controls at 0–1 cm layer; modified original data to exclude the	160 $\pm$ 45.15	17
<b>ECHO</b>	Wilson & Hessler, 1987	77.29 $\pm$ 55.19	7	Foraminifera, Protozoa and Calanoida	77.29 $\pm$ 55.19	7
<b>BGR_RA</b>	Martínez Arbizu & Haeckel, 2015; Hauquier et al., 2019	483.84 $\pm$ 95.18	5	abundance and s.d. obtained from Hauquier et al., 2019; number of deployments obtained from Martínez Arbizu & Haeckel, 2015	483.84 $\pm$ 95.18	5
<b>OMS</b>	This study	235.73 $\pm$ 26.39	12		235.73 $\pm$ 26.39	12
<b>COMRA West</b>	Gao et al., 2002	18.05	10	used 18.05 for calculations	29.16 $\pm$ 15.7	2
	Wang et al., 2013	40.26 $\pm$ 25.84	6	used the average: 40.26		
<b>COMRA East</b>	Gao et al., 2002	32.47	10	used 32.47 for calculations	68.44 $\pm$ 50.86	2
	Wang et al., 2013	104.40 $\pm$ 20.48	6	used the average: 104.40		
	Mahatma, 2009	181.66 $\pm$ 35.56	Five stations sampled, total of eight corers	outside nodule area; used the average: 181.66 for calculations	153.26 $\pm$ 49.62	3
<b>IFREMER</b>	Mahatma, 2009	95.97 $\pm$ 23.43	Five stations sampled, total of eight corers	nodule area; used the average: 95.97 for calculations		
	Martínez Arbizu & Haeckel, 2015; Hauquier et al., 2019	182.15 $\pm$ 62.42	5 deployments	used the average: 182.15 for calculations		

		46.2–205.3		Baseline studies from five box cores, two subcores taken from each box core samples	took the average of min (46.2) and max (205.3) to get: 125.75		
<b>NOAA-BIE</b>	Radziejewska, 2014					95.88 ± 42.24	2
		40.74–91.28		Five control multicorer samples	took the average of min (40.74) and max (91.28) to get: 66.01		
	Pape et al., 2017	106.6 ± 29.3	3		used the average: 106.6		
	Pape et al., 2017	88.1 ± 55.0	3		used the average: 88.1		
<b>GSR (B4)</b>	Pape et al., 2021	126.8 ± 29.0	4		used the average: 126.8	90.78 ± 30.12	5
	Pape et al., 2021	87.0 ± 21.0	4		used the average: 87.0		
	Pape et al., 2021	45.4 ± 31.5	3		used the average: 45.4		
	Martínez Arbizu & Haeckel, 2015; Hauquier et al., 2019	211.49 ± 40.36	5 deployments		used the average: 211.49		
<b>GSR (B6)</b>	Pape et al., 2017	<b>242.3 ± 59.2</b>	4		used the average: 242.3	201.63 ± 46.39	3
	Pape et al., 2017	151.1 ± 54.2	3		used the average: 151.1		
	Radziejewska, 2002	100.66					
	Radziejewska, 2002	105.7					
	Radziejewska, 2002	245.14	6		averaged this (C1) to become 201.6		
	Radziejewska, 2002	86.1					
	Radziejewska, 2002	277.76					
	Radziejewska, 2002	394.24					
	Radziejewska, 2002	244.56					
<b>IOM-BIE</b>	Radziejewska, 2002	198.94	3		averaged this (C2) to become 198.79	236.73 ± 182.45	5
	Radziejewska, 2002	152.88					
	Radziejewska & Modlitba, 1999; Radziejewska, 2014	91.56 ± 23.31	3		nodule bearing area; abundance data taken from Radziejewska (2014). Used the average: 91.56		
	Radziejewska et al., 2001	138.97 ± 3.49	3		control only (C3); used the average: 138.97		
	Martínez Arbizu & Haeckel, 2015; Hauquier et al., 2019	552.71 ± 260.32	3 stations, 3 deployments		used the average: 552.71		
	Martínez Arbizu & Haeckel, 2015; Hauquier et al., 2019	371.84 ± 33.11	5		used the average: 371.84		
<b>BGR_PA</b>					calculated average from supplementary data in Uhlenkott et al. (2020); used the average: 306.62	339.23 ± 46.12	2
	Uhlenkott et al., 2020	306.62 ± 98.95	106				

1034  
1035  
1036  
1037  
1038  
1039  
1040  
1041  
1042  
1043  
1044  
1045

1046  
1047  
1048  
1049**Table S6.**

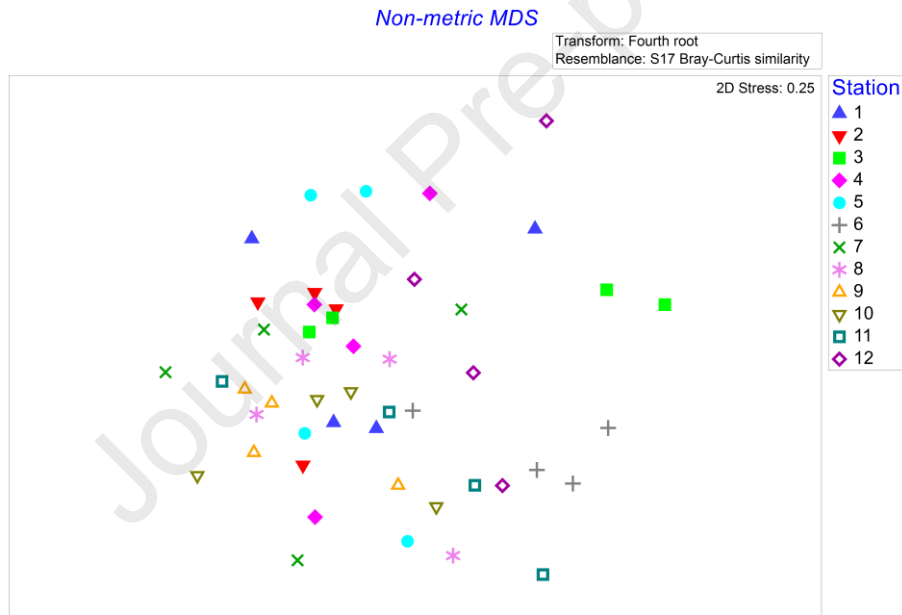
PERMANOVA main test results and significant pair-wise comparisons ( $P(\text{MC}) \leq 0.05$ ) among the 12 stations (0–5 cm sediment layer) in the OMS area of the CCFZ using relative abundances, when analysing the four cores taken from each deployment at each station separately.

PERMANOVA main test

Source of variation	df	SS	MS	Pseudo-F	$P(\text{perm})$	perms	$P(\text{MC})$
Station	11	3534.40	321.31	2.27	< 0.01	9863	< 0.01
Residual	36	5106.10	141.84				
Total	47	8640.60					

Pair-wise comparisons

Groups	$t$	$P(\text{MC})$	Unique perms
1, 6	1.89	0.05	35
2, 6	2.56	0.01	35
3, 9	2.18	0.03	35
3, 10	1.85	0.04	35
4, 6	1.99	0.03	35
5, 6	2.61	0.01	35
5, 9	2.16	0.02	35
5, 10	1.85	0.04	35
6, 7	1.97	0.03	35
6, 8	2.42	0.02	35
6, 9	2.65	0.01	35
6, 10	2.10	0.03	35

1050  
1051  
10521053  
1054  
1055  
1056

**Fig. S1.** Non-metric dimensional scaling (nMDS) of 12 stations (0–5 cm sediment layer) in the OMS area of the CCFZ, including four cores taken from each deployment at each station. Symbols and numbers represent the 12 stations and replicates.

**Community structure of deep-sea benthic metazoan meiofauna in the polymetallic nodule fields in the eastern Clarion-Clipperton Fracture Zone, Pacific Ocean**

**HIGHLIGHTS**

- Provides the first quantitative description of meiofaunal composition in the OMS contract area (eastern CCFZ)
- Community structure was different at 12 randomly sampled stations within a  $30 \times 30$  km area, confirming that the meiofauna residing in the CCFZ deep sea floor is very diverse
- Substratum shear strength was significantly associated with differences in meiofaunal abundance and community structure
- Our findings reiterate the decreasing westward trend of meiofaunal abundance in the CCFZ

**Declaration of interests**

The authors declare that they have no known competing financial interests or personal relationships that could have appeared to influence the work reported in this paper.

The authors declare the following financial interests/personal relationships which may be considered as potential competing interests:

Journal Pre-proof